Pituitary stem cells differ according to their position in the gland and maintenance of their progeny depends on physiological context.

Running Title: Pituitary stem cell heterogeneity and regeneration

Karine Rizzoti[a,1], Probir Chakravarty[b], Daniel Sheridan[a], and Robin Lovell-Badge[a,1].

[a] Laboratory of Stem Cell Biology and Developmental Genetics, The Francis Crick Institute, London NW1 1AT, UK
[b] Bioinformatics core, The Francis Crick Institute, London NW1 1AT, UK
[1] authors for correspondence karine.rizzoti@crick.ac.uk and robin.lovell-badge@crick.ac.uk

ABSTRACT

Stem cell (SC) differentiation and maintenance of resultant progeny underlie regeneration in many organs, but it is difficult to pinpoint contribution of either process. In the pituitary, a central regulator of endocrine axes, a population of adult SCs undergo activation following target organ ablation, providing a well-characterized paradigm to study regeneration in a multi-organ system. Here we used single cell technologies to characterize SC heterogeneity and regeneration modalities. We consequently performed lineage tracing experiments. Our result show that SC differentiation occurs more frequently than previously thought. In regenerative conditions, differentiation is both increased and more diverse than lineage tracing experiments demonstrated. Detailed examination of SC progeny demonstrate that nascent cells maintenance is an important regulatory step controlling SC-derived regeneration, highlighting a trophic role for the microenvironment. Analyses of cell trajectories further predict modalities, and potential new players involved in regeneration. Our model provides a unique system to study the influence of evolving physiological states on the mechanisms of SC regeneration.

Teaser: Pituitary stem cells are heterogeneous and differentiate more than formerly thought but maintenance of their progeny is selective.

INTRODUCTION

The pituitary gland controls the three major endocrine axes, reproduction, stress and metabolism, and is involved in homeostasis; all under control of the hypothalamus. Its function requires modulation of hormonal output over short and long terms, and this is regulated at several levels, including rates and patterns of hormone secretion, synthesis and storage, and changes in endocrine cell numbers. Two different mechanisms are known to underlie endocrine cell emergence: division of endocrine cells and differentiation from resident SCs. Under normal and stable conditions, it is thought that division from endocrine cell types is sufficient for the typical low cell turnover seen in the pituitary (1). This has been directly shown in corticotrophs using a genetic trick where cell division induces apoptosis of POMC expressing cells. A gradual loss of corticotrophs is observed in these pituitaries in support of the role of these endocrine cells in their own replacement (2). In agreement, long term lineage tracing of adult SOX2 and SOX9 +ve pituitary SCs in steady-state conditions suggests that SCs differentiate rarely and thus do not significantly participate in cell turnover (3) (4). Furthermore, adult ablation of the SCs does not appear to affect pituitary function (5). In contrast, when the regenerative potential of the gland is stimulated, either by endocrine cell ablation (6) or target organ ablation (3), SC-derived new endocrine cells of the appropriate type emerge. In this latter paradigm, differentiation from SCs appears to be the main process underlying emergence of new corticotrophs after adrenalectomy (Ax) (2), providing a well characterized multi-organ system to explore mechanisms of regeneration.

Here, we explore the characteristics of pituitary SC fate acquisition using single cell approaches combined with lineage tracing analyses. We observe that SOX9 +ve pituitary SCs comprise several functionally distinct sub-populations, located in the ventral and dorsal part of the epithelium lining the pituitary cleft and in the anterior pituitary parenchyma. We then explored mechanisms underlying SC mobilization following target organ ablation through characterizing cell trajectories and GRNs potentially involved in cell fate acquisition. We observed that while fate acquisition of the targeted cell type (corticotrophs after Ax and gonadotrophs after gonadectomy) was efficiently induced, differentiation toward all endocrine cell types unexpectedly also took place. Examination of longer-term outcomes using lineage tracing further showed that only a proportion of the differentiated progeny is retained, specifically that of the targeted cell type. More precisely, we only observe SC-derived corticotrophs after Ax, and lactotrophs in females, likely highlighting oestrogen involvement. Therefore, while pituitary SC differentiation appears both more frequent and diverse than previously thought, our results suggest that the selective maintenance of nascent cells, according to perceived physiological need and likely sex-dependent hormonal cues, is an important regulatory step controlling the regenerative response from SCs. Our model thus allows characterisation of this response following pathophysiological manipulations that may well relate to normal life-changing events, such as puberty, pregnancy and lactation.

RESULTS

Distinct regulatory pathways govern AL and IL SC identity

The anterior lobes of three *Sox9*$^{iresGFP/+}$ adult male pituitaries were dissociated and the transcriptome of single GFP +ve cells analysed after fluorescence activated cell sorting (FACS), as previously described (3). After quality checks, 1993 cells were retained for further analysis; clustering was performed by generating UMAP plots. Three major clusters were identified (Fig.1A). Co-expression of *Sox2* and *Sox9* in clusters 0 and 2 (Fig.1B), representing 69% of the cells, suggested that these were likely to represent SCs. The remaining cluster (1), representing 24% of the dataset, comprised cells where *Sox*9 was detected, but where *Sox2* was greatly reduced or absent. Finally, cells each expressing a different hormone and the corresponding lineage specifying factors, were grouped within a single smaller cluster (3) representing 3% of the cells (Fig.1B). SOX9 is not expressed in any endocrine cell in quiescent conditions (7). However, we observed some rare SOX9;ACTH +ve cells, and more numerous GFP;ACTH +ve cells in *Sox9*$^{iresGFP/+}$ animals exclusively after activation of the SCs by pituitary target organ ablation (3) (Sup. Fig.1). This suggests that differentiating, and recently differentiated cells are present in the SOX9iresGFP fraction due to persistence of the GFP. Therefore, the cells present in cluster 3 are likely to represent cells committed toward an endocrine fate, with the largest population (41% of cluster 3 cells) expressing *Prolactin*.

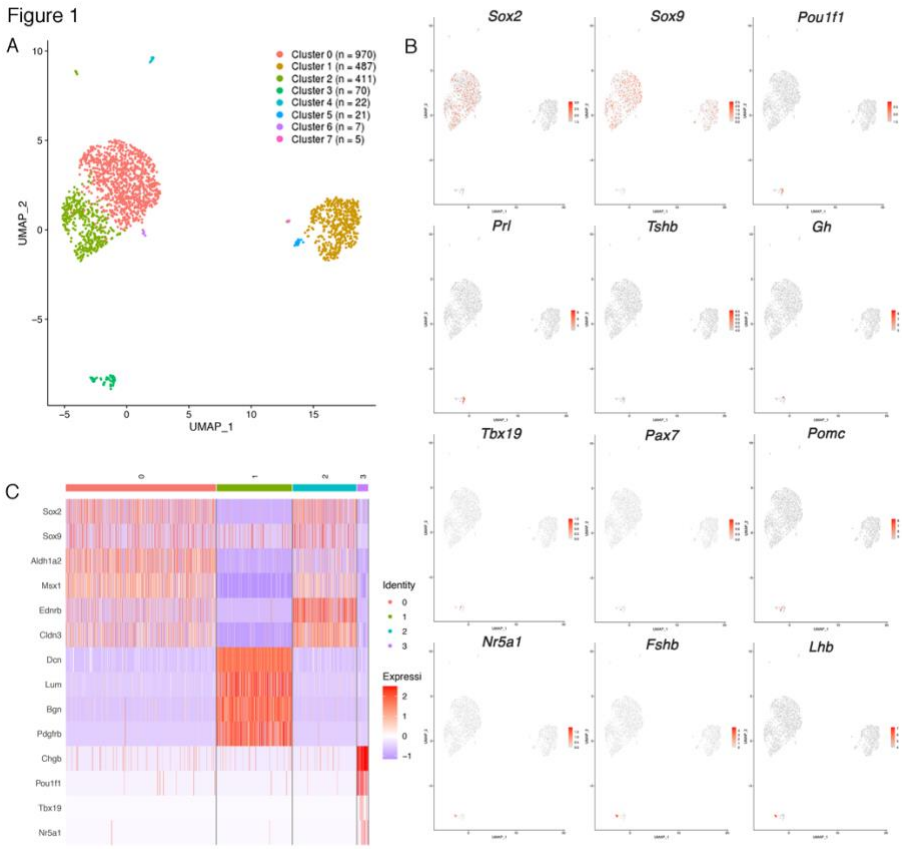

Figure 1: Single cell analysis of the *Sox9*$^{iresGFP/+}$ population in male pituitaries.

A) UMAP clustering of *Sox9*$^{iresGFP/+}$ cells.
B) *Sox2* and *Sox9* were used to identify SCs (7) while genes encoding for hormones (*Gh*, *Prl*, *Tshβ*, *Lhβ*, *Fshβ*, *Pomc*) and lineage specific transcription factors were examined to distinguish committed cells (*Pou1f1* for somatotrophs, lactotrophs and thyrotrophs, *Tbx19* and *Pax7* for corticotrophs and melanotrophs, and *Nr5a1* for gonadotrophs).
C) Heatmap displaying the top markers for the main clusters.

The two SC clusters were further explored. Analysis of differentially expressed genes (DEG) (Fig.1C) shows that clusters 0 and 2 are relatively similar and are distinguished by differences in levels of expression of specific genes. *Aldh1a2*, encoding for an enzyme involved in retinoic acid (RA) synthesis, and the transcription factor *Msx1* were preferentially present in cluster 0, while *Ednrb*, encoding for the endothelin B receptor, and the cell adhesion molecule *Claudin3* were both expressed at higher levels in cluster 2. RA is required during pituitary morphogenesis (8) (9) and *Msx1* interacts with SOX2 for *Prop1* regulation (10), while nothing is known about *Ednrb* or *Claudin3* in pituitary SCs. In the gland, expression of the four markers is restricted to SCs (Fig.2). In the epithelium lining the cleft, cluster 0 markers ALDH1a2 and MSX1 are expressed exclusively on the AL side (Fig.2 A,B), while cluster 2 markers EDNRB and CLAUDIN-3 (Fig.2 C,D) are present on both sides. In the parenchyma ALDH1a2, MSX1 and CLAUDIN-3 co-localise with SOX2/9 while expression of EDNRB is not detectable. These results suggest that cluster 0 is enriched in anterior lobe SCs, while cluster 2 has a more generic pituitary SC identity.
Pathway analysis in cluster 0 (Sup Table.1) highlighted activity of the NOTCH and WNT pathways and presence of Ephrin signalling, as previously reported in pituitary SCs (11) (12). Cluster 2 cells are characterised by expression of cytoskeleton remodelling and adhesion genes consistent with the EMT-like process required during pituitary progenitor cell fate acquisition (13). In conclusion, regionalisation of these two SC subpopulations is functionally underlined by the activity of specific regulatory pathways.

Folliculo-stellate (FS) cells are specialised AL glial cells (14). These express S100b in the rat, but not in the mouse ((15, 16), Sup. Fig.2). To clarify their relationship with SCs, we examined expression of *Aldolase C* (16) and of *Slc152a*, which encodes a transporter responsible for the FS specific import of AMCA (17). Both are selectively present in SCs, in clusters 0 and 2, implying that in the mouse FS and SCs are overlapping populations.

In conclusion, single-cell analysis of the *Sox9*$^{iresGFP/+}$ pituitary fraction successfully resolved heterogeneity of this population, suggesting differential activity of new pathways, and clarified the relationship between SC with the FS cells.

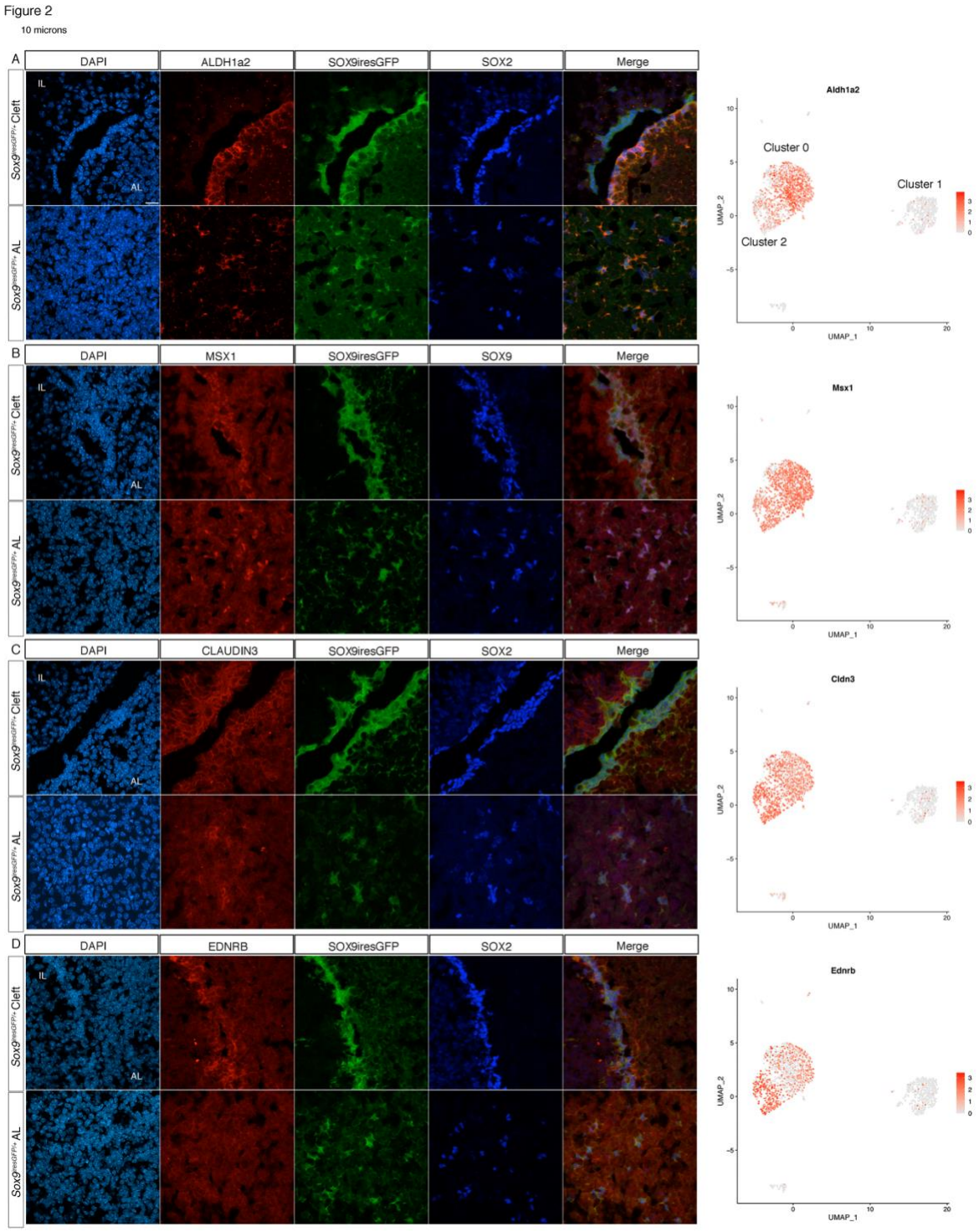

Figure 2: Differential expression of SC cluster markers.

A) Co-immunofluorescence for ALDH1A2, GFP and SOX2 in a male SOX9iresGFP pituitary section. ALDH1A2 is exclusively expressed in SOX2;SOX9 AL SC. *Aldh1a2* UMAP shows enrichment in cluster 0.

B) Co-immunofluorescence for MSX1, GFP and SOX9 in a male SOX9iresGFP pituitary section. MSX1 is exclusively expressed in SOX2;SOX9 AL SC. *Msx1* UMAP shows enrichment in cluster 0.

C) Co-immunofluorescence for CLAUDIN3, GFP and SOX2 in a male SOX9iresGFP pituitary section. CLAUDIN3 is exclusively expressed in SOX2;SOX9 SC. *Cldn3* UMAP shows enrichment in cluster 2.
D) Co-immunofluorescence for EDNRB, GFP and SOX2 in a male SOX9iresGFP pituitary section. EDNRB is exclusively expressed in SOX2;SOX9 cleft SC. *Ednrb* UMAP shows enrichment in cluster 2. Similar expression profiles were observed in females for all markers. The scale bar in A represents 10 μm for all panels.

A novel population of parenchymal SOX9;PDGFRβ +ve cells

Cluster 1, representing 25% of the cells, is characterised by expression of PDGFRβ (Fig.1C). *In situ*, PDGFRβ;SOX9 +ve cells are exclusively detected in the parenchyma. Expression of SOX9 in these double +ve cells is weaker than in SCs (Fig.3A) and SOX2 is not detected in them (Fig.1B and 3B). In contrast with the *in silico* analysis, only 8±1.62% SD of parenchymal SOX9 +ve cells express PDGFRβ in males (Fig.3C). This discrepancy could be due either to an over-representation of cluster 1 cells, because epithelial SCs are more difficult to recover than parenchymal cells, or to the difficulty in detecting the cells by immunofluorescence. We observe significantly fewer PDGFRβ;SOX9 +ve cells in females than in males (1.3±0.6% SD, p= 0.029, Fig.3C). PDGFRβ +ve pituitary cells are known to comprise a mural vascular network (15), and in agreement, some SOX9;PDGFRβ cells display a pericyte like morphology (Fig.3D). In the embryo, vascular and mural cells have an extra-Rathke's pouch origin, as they emerge from immigrating neural crest cells (18, 19). Because cluster 1 cells do not express the generic pituitary marker *Pitx1* (Fig.3E), we analysed a potential neural crest origin by performing WNT1-Cre lineage tracing. 79 ± 3.1% SEM of SOX9;PDGFRβ cells (n=130 cells from 4 males) derive from WNT1-Cre +ve cells (Fig3C, F) while in females only 47.5 ± 5.5% SEM of the cells derive from the neural crest (n= 38 cells from 2 females, p= 0.036). Therefore, we propose that cluster 1 cells represent a sexually dimorphic mural network with a dual embryonic origin.

Figure 3

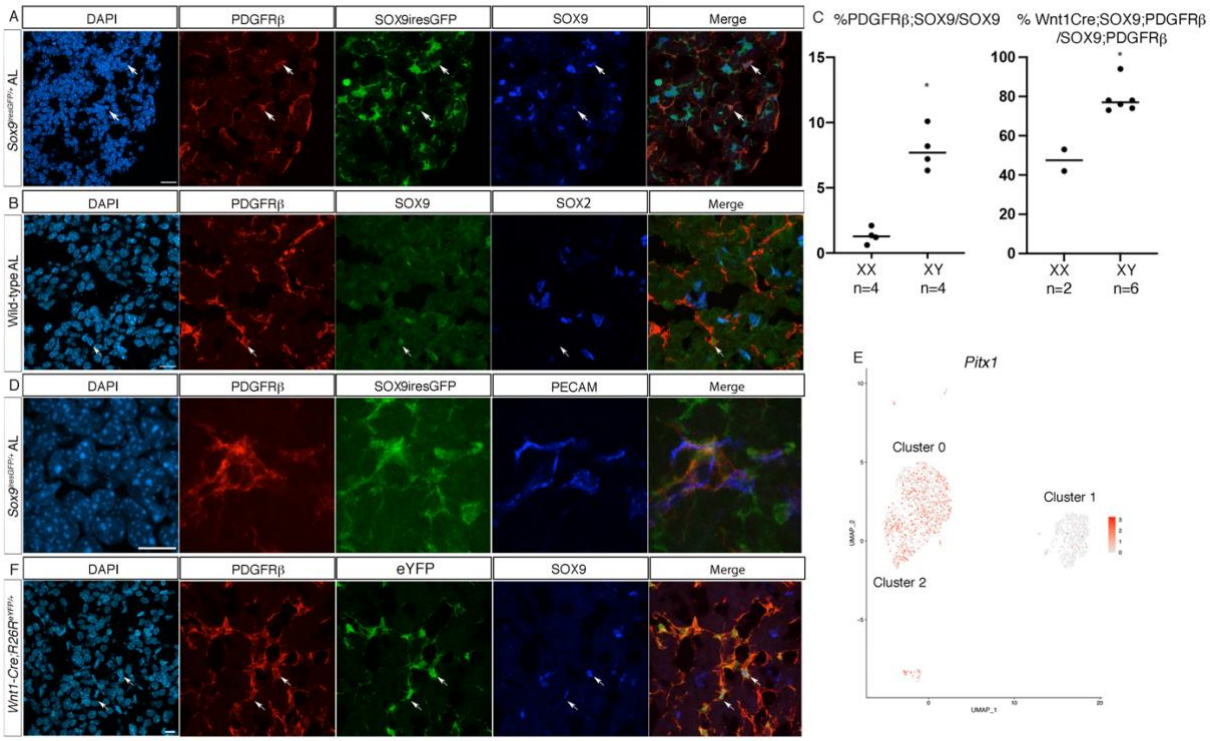

Figure 3: Characterisation of a SOX9;PDGFRβ +ve AL cell population.

A) Co-immunofluorescence for PDGFRβ, GFP and SOX9 in a Sox9iresGFP AL section. Triple +ve cells are indicated (arrows).

B) Co-immunofluorescence for PDGFRβ, GFP and SOX2 in AL. A SOX9;PDGFRβ +ve cell which is negative for SOX2 (arrow).

C) Percentage of GFP;SOX9;PDGFRβ/GFP;SOX9 +ve cells in *Sox9iresGFP* male and female AL sections (average 500 SOX9 cells counted/animal, $p = 0.029$). Percentage of SOX9;PDGFRβ +ve cells of neural crest origin ($p = 0.036$; Mann Whitney test).

D) Co-immunofluorescence for PDGFRβ, GFP and PECAM in a Sox9iresGFP AL section showing a SOX9;PDGFRβ +ve cell resembling a pericyte bridging PECAM +ve capillaries.

E) UMAP for *Pitx1*.

F) Co-immunofluorescence for PDGFRβ, eYFP and SOX9 in a *Wnt1-Cre;R26R*^{eYFP} AL section. Triple +ve cells are shown (arrows).

The scale bars represent 10 µm.

All endocrine cell types are present in the *Sox9*$^{iresGFP/+}$ +ve compartment after SC mobilization

We then performed sc-RNAseq on activated SCs. Target organ ablation induces a transient proliferative wave in the gland, mostly affecting SCs, which can then give rise to new endocrine cells (2, 3, 20). We analysed the transcriptome of *Sox9*$^{iresGFP/+}$ male cells 4 days after removing the adrenals, the testes or both. We selected an average of 50% extra cells compared to our previous dataset (about 1.5% of the whole population) to include cells expressing GFP weakly, and thus potentially differentiating. We integrated these datasets with that obtained from

unchallenged animals and obtained a similar clustering of SCs (Fig.1, Fig.4A,B, Sup. Fig.3A). A pairwise comparison for proportion test limited to SC clusters, comparable across all the datasets since they express high levels of GFP, demonstrates a significant increase in proliferative cells after target organ ablation, as previously shown (3). We also observe the emergence of distinct hormone +ve clusters representing in total 25 to 30% of all cells (Fig.3A,B). Target organ ablation is associated with increased secretion, and sometimes cell numbers, of the endocrine population regulating the resected organ. However, regardless of the glands removed, all endocrine cell lineages emerge in the Sox9iresGFP +ve fraction. While we expected *Pomc* +ve cells to prominently feature after Ax, these were outnumbered by *Prl* and *LHb*;*FSHb* +ve cells (Sup. Fig. 3C). Similarly, gonadectomies were expected to trigger commitment toward the gonadotroph cell fate, but *Gh* +ve cells were mostly observed. To characterise these *Sox9*$^{iresGFP/+}$;hormone +ve cells we compared them with endocrine cells by integrating our datasets with one from whole pituitaries (21). *Sox9*$^{iresGFP/+}$;hormone +ve cells cluster with endocrine cells (Fig.4C, D). Therefore, they represent differentiated cells, at least transcriptionally. In conclusion, target organ ablation induces differentiation of SCs, but there is an unexpected lack of specificity in the endocrine cell types produced, with all hormonal markers being up-regulated.

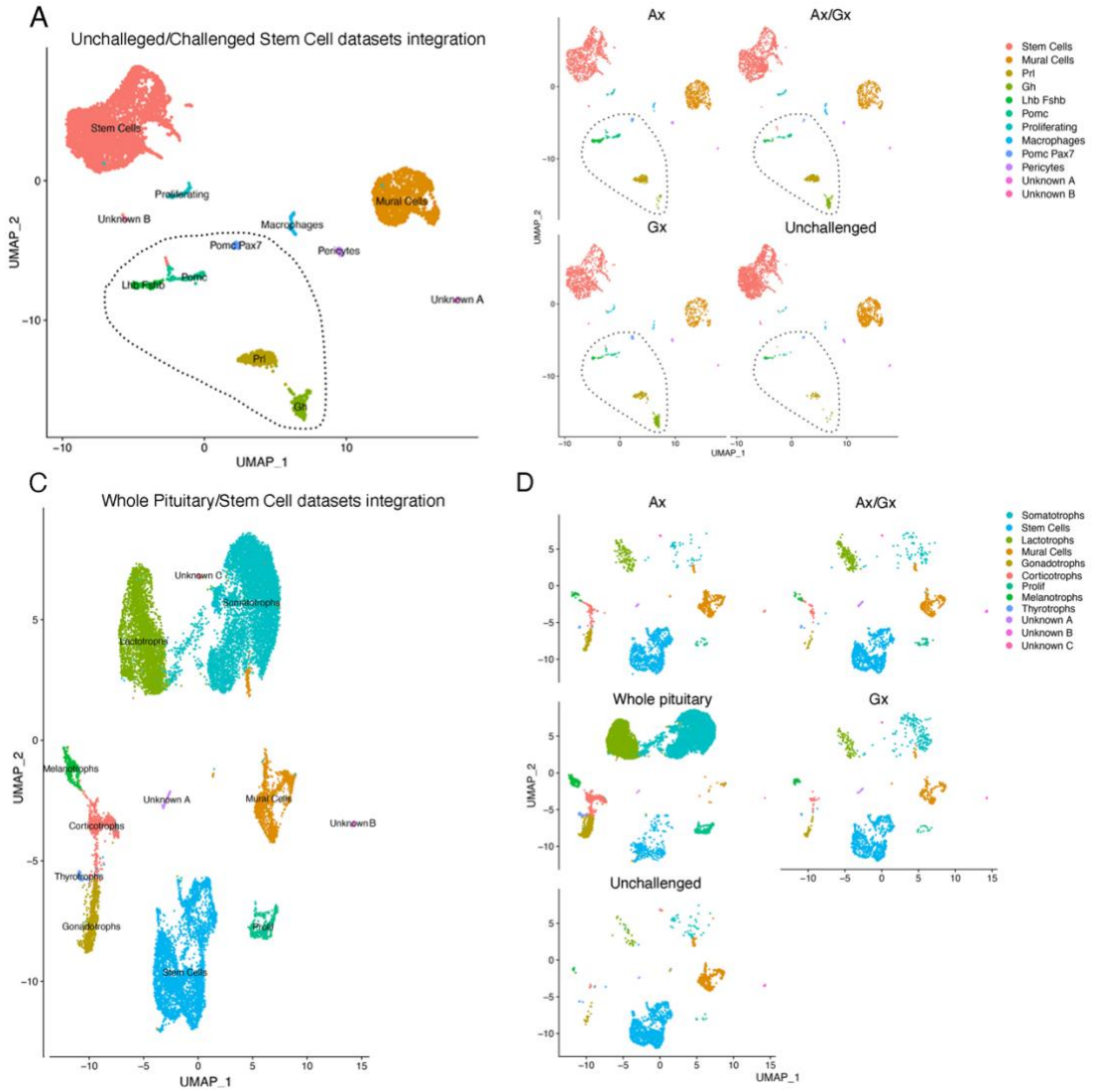

Figure 4: Target organ ablation induces differentiation toward multiple endocrine lineages.
A) UMAP clustering for integrated datasets from sorted *Sox9*$^{iresGFP/+}$ cells from unchallenged, adrenalectomized, gonadectomized and both adrenalectomized and gonadectomized animals, 4 days after surgery. B) UMAP clustering split by experiment. Cells expressing all pituitary hormones are present (dotted lines) in all conditions. C) UMAP clustering for integrated datasets from sorted *Sox9*$^{iresGFP/+}$ cells and a whole pituitary dataset (21). D) UMAP clustering split by experiment show that hormone +ve cells present in the *Sox9*$^{iresGFP/+}$ cells cluster with endocrine cells.

Analyses of cell trajectories after Ax.

We decided to focus on Ax because it represents the most efficient stimulus of SC differentiation after target organ ablation (3). We added a new time point at day 2 after Ax and a sham control. More cells were collected (about 2% of the whole AL population) and sequenced in these new datasets (5000 and 6000 cells) which were integrated (Fig.5A) with our initial dataset (Fig.1) and the one performed 4 days after Ax (Fig.4). UMAP clustering indicated that SCs were present in four distinct clusters (Sup. Fig.4). In addition to the *Ednrb* and *Aldh1a2* clusters, two SC clusters (SC3 and SC4) emerged (Fig.5A). These were mostly populated by cells from the new datasets (Sup. Fig.5). SC3 was characterised by higher expression of markers also present in the *Ednrb* and *Aldh1a2* clusters. SC4, mostly derived from the Ax+48h00 dataset, showed co-expression of SC and endocrine markers suggesting that it represents cells in a transitioning phase (Sup. Fig.4). Finally, endocrine cell clusters were detected (Sup. Fig.4), as observed previously (Fig.4).
In sham operated animals, 4.5% of hormone expressing cells, mostly *Prl* +ve, were present, confirming our observations in unchallenged animals (Sup. Table 2). 48 hours after Ax, the proportion of hormone +ve cells had increased to 11%, and this had doubled after 4 days. Because expression of Sox9iresGFP depends on *Sox9* and is thus not cumulative, as in classical lineage tracing experiments, this increasing proportion means that commitment toward differentiation augments in the 4 days following ablation. A pairwise proportion test between the 2 new datasets, sorted identically on the same day, showed that a shift occurs from SC4 where the proportion of cells from the Ax dataset is significantly increased, fitting with its transitioning phase profile (Fig.5B, Sup. Fig.4). At this shorter time point, 48 h00 after adrenal ablation, corticotrophs are the most significantly increased cell type, while 4 days after surgery they were outnumbered by lactotrophs. This sharp and transient increase could represent the specific SC response to adrenal ablation.

We then performed trajectory analyses after principal component analysis (PCA) using Slingshot (22). Trajectories finishing at each endocrine cell type were discovered, with a common root through SC clusters *Ednrb*, *Aldh1a2,* proliferative cells and SC4, then ending at each endocrine cell type (Fig.5C, Sup. Fig.6). In the corticotroph trajectory (Fig.5D), the expression pattern of 2245 genes significantly correlates with pseudotime (Fig.5E). The expression of known SC markers (*Ednrb*, *Sox2*, *Sox9*, *Aldh1a2*) and signalling pathway members (*Notch2*, *Hes1*, *Hey1* and *Wnt4*, *Fzd2*, *Sfrp5*) was gradually lost. Pathway analyses

further suggest keratin filament remodelling, in agreement with epithelial to parenchymal transition during differentiation. *Ismn1* (23) and *Prop1*(13), which are involved in cell fate acquisition, are also present during early phases. Conversely, the corticotroph specifier and marker genes *Neurod1*, *Ascl1*, *Tbx19*, *Pomc* and *Creb3l2* (24) are upregulated as cells differentiate. A sharp transition occurs as *Prop1* is upregulated and is characterised by a transient up-regulation of *Pou1f1* lineage and gonadotroph (*Fshb*) genes. This could reflect permissive chromatin remodelling as endocrine cell fate acquisition occurs.

SCENIC analysis was then performed to explore GRNs (25) (Fig.5G). As expected *Sox2* and *9* regulons featured in SC clusters while *Ascl1*, *Neurod1* and *Creb3l2* were present in corticotrophs. The thyroid (*Thra*) and the androgen (*Ar*) hormone receptor regulons featured in differentiating SCs, suggesting that SCs can respond to peripheral signals. New pituitary GNRs were also discovered, such as those involving *Runx1* and *Irf9* whose expression was validated in SCs (Fig.5G, E). RUNX1 (RUNt-related transcription tactor 1) is known to control adult skin SC maintenance by regulating WNT signalling (26), whereas IRFs (Interferon Regulatory Factors) are modulators of cell growth and differentiation beside their anti-viral functions. IRF9 associates with phosphorylated STAT1:STAT2 (Signal Transducer and Activator of Transcription) dimers, which are both present in our analysis (27). Finally, several RA factors were present, supporting RA involvement during endocrine cell differentiation.

In conclusion, by adding new datasets, we validated our previous observations suggesting a low differentiation rate of SCs, mostly into lactotrophs in the intact animals. We refined the dynamics of the regenerative response after mobilization, showing a transient peak of corticotroph differentiation 48 hours after Ax and, importantly, we were able to infer cell trajectories.

Figure 5

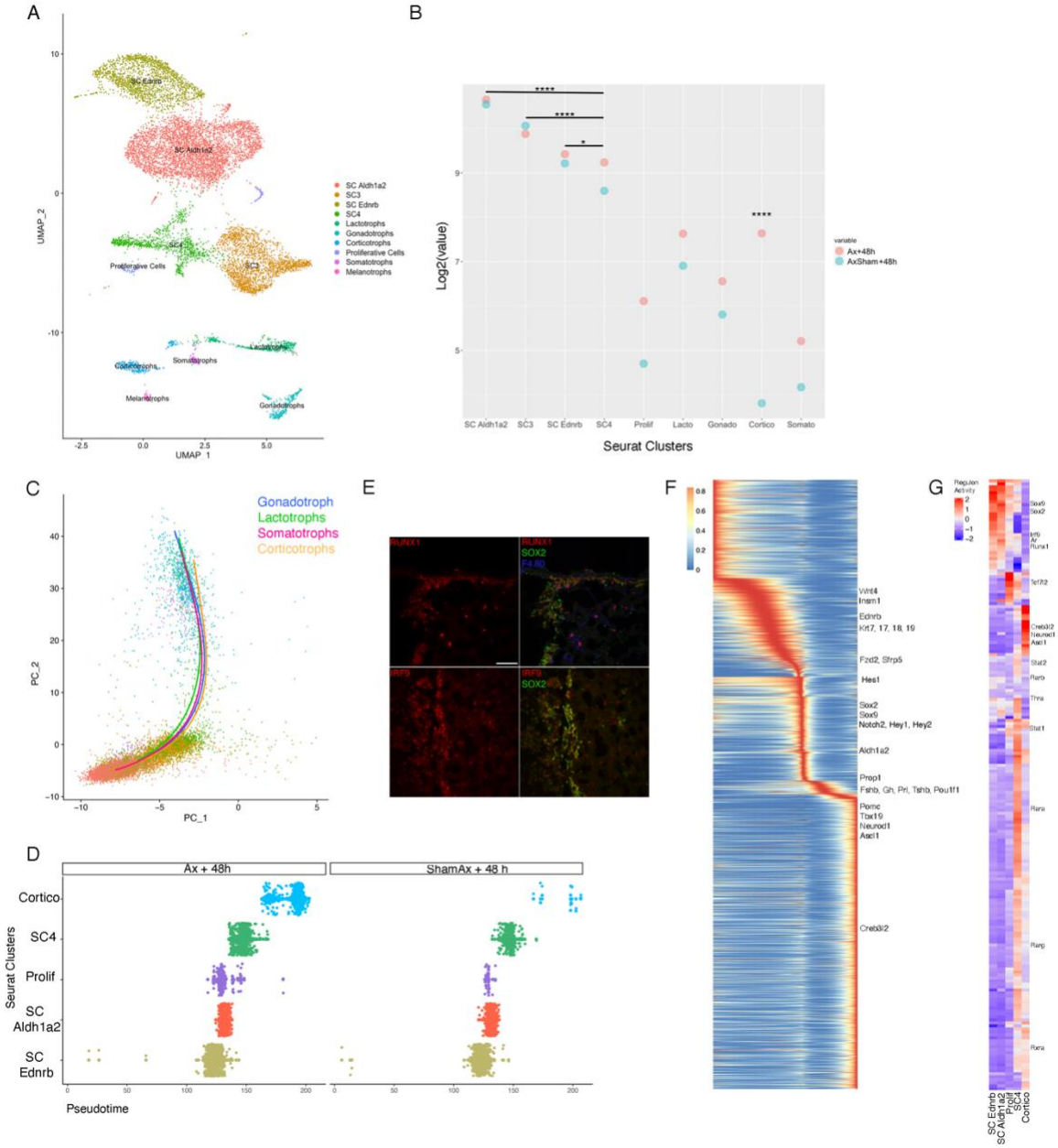

Figure 5: Trajectory analyses following Ax.

A) UMAP clustering for integrated datasets from sorted GFP +ve cells from unchallenged, adrenalectomized and sham + 48 h, and + 4 days, all from *Sox9*$^{iresGFP/+}$ pituitaries. The data has been filtered to remove mural and vascular cells and outliers. Cluster colour scheme is constant throughout the figure. B) Pairwise comparison for proportion test performed on adrenalectomized and sham + 48h. The proportion of corticotrophs after Ax is significantly different from all other cluster distributions. The proportion of cells in cluster SC4 is significantly different from all other SC cluster distributions (Sup. Table2). C) Representation of endocrine cell trajectories on the PCA plot for integrated dataset. D) Proportion of cells/cluster in the corticotroph trajectory comparing Ax and sham Ax. Differentiation is occurring predominantly after Ax. E) Immunofluorescence on pituitary sections validates RUNX1 and IRF9 expression in SOX2 +ve SCs. RUNX1 is also expressed in F4.80 +ve macrophages. F) Heatmap of 2245 genes associated with the corticotroph trajectory. G) Heatmap of SCENIC analysis on the corticotroph trajectory.

Selective maintenance of SC progeny

To examine predictions from our transcriptomic analyses, we performed two different types of lineage tracing experiment. First, we directly assessed expression of hormonal markers on plated *Sox9*$^{iresGFP/+}$ FACSorted single cells by immunofluorescence in males and females, 4 days after Ax or sham-surgery. Second, to follow mobilized SCs further, we used *Sox9*$^{ires\text{-}CreERT2/+}$; *R26R*$^{EYFP/+}$ animals and examined progeny 10 to 11 days after Cre induction (a week after surgery since induction is mostly performed for 3 days before surgery).

All hormone +ve cell types were found in the GFP +ve fraction in both experimental and control animals, which matches our transcriptomic analyses (Fig.6 A, B). Following Ax, the number of POMC +ve cells increased the most, in agreement with our earliest dataset (Ax+ 48h). However, even if less efficiently stimulated, the proportion of most other endocrine cell types was comparable to that of corticotrophs. This again reflected our transcriptomic data. More precisely, we also observed a slight increase in somatotroph emergence in both sexes, while lactotrophs appear to increase only in females; and the low LH +ve cell numbers are not affected by target organ ablation.

We then carried out lineage tracing in *Sox9*$^{ires\text{-}CreERT2/+}$; *R26R*$^{EYFP/+}$ animals (Fig.6C). In contrast with our previous results (Fig.6A), examination of pituitary sections exclusively revealed the presence of POMC;eYFP +ve corticotrophs after Ax, in comparable numbers in both sexes (Fig.6C). In females, we additionally observed lactotrophs, and did so even without performing target organ ablation. Quantification of lactotroph emergence on dissociated pituitaries confirmed the sex bias (Fig.6D). Correcting for CreERT2 induction efficiency, we estimate that in females SCs contribute to 0.6% of the total population of lactotrophs and these SC-derived lactotrophs represent 2% of the eYFP +ve population (Fig.5F).

The two genetic tools we used, *Sox9*^{iresGFP} and *Sox9*$^{ires\text{-}CreERT2/+}$, display inherent distinctions, such as use of high-dose of the Selective Estrogen Receptor Modulator (SERM) tamoxifen, and purposes, where these may impair direct comparisons. However, while results from both transcriptomic analyses and immunofluorescence demonstrate that endocrine cells of all types are produced in comparable numbers in the short term, we clearly observe that corticotrophs are the only endocrine cells remaining in long-term lineage tracing experiments in males. This indicates a selective maintenance of nascent endocrine cells.

To further explore the sex bias in SC-derived lactotrophs, we administered tamoxifen to P0 *Sox9*$^{ires\text{-}CreERT2/+}$; *R26R*$^{EYFP/+}$ pups and quantified differentiation into lactotrophs once they reached adulthood. There was no significant difference in the proportion of SC-derived lactotrophs between males and females (Fig.5E), as previously observed (3). Therefore, male SC-derived lactotrophs can be produced, but this is temporally restricted. Furthermore, because the proportion of lactotrophs generated from male and female pups is similar, this suggests that tamoxifen, which can interfere with estrogen action, induces lactotroph emergence. If lactotroph emergence was a continuous process in females their proportion would have been far superior to that observed in males. Our results thus reveal a temporal window of sensitivity in males, while female SCs remain responsive to the lactotroph promoting effect of tamoxifen

until adulthood. It is unclear how E2 signalling is altered, and whether SC differentiation is induced or maintenance of nascent lactotrophs permitted.

Figure 6

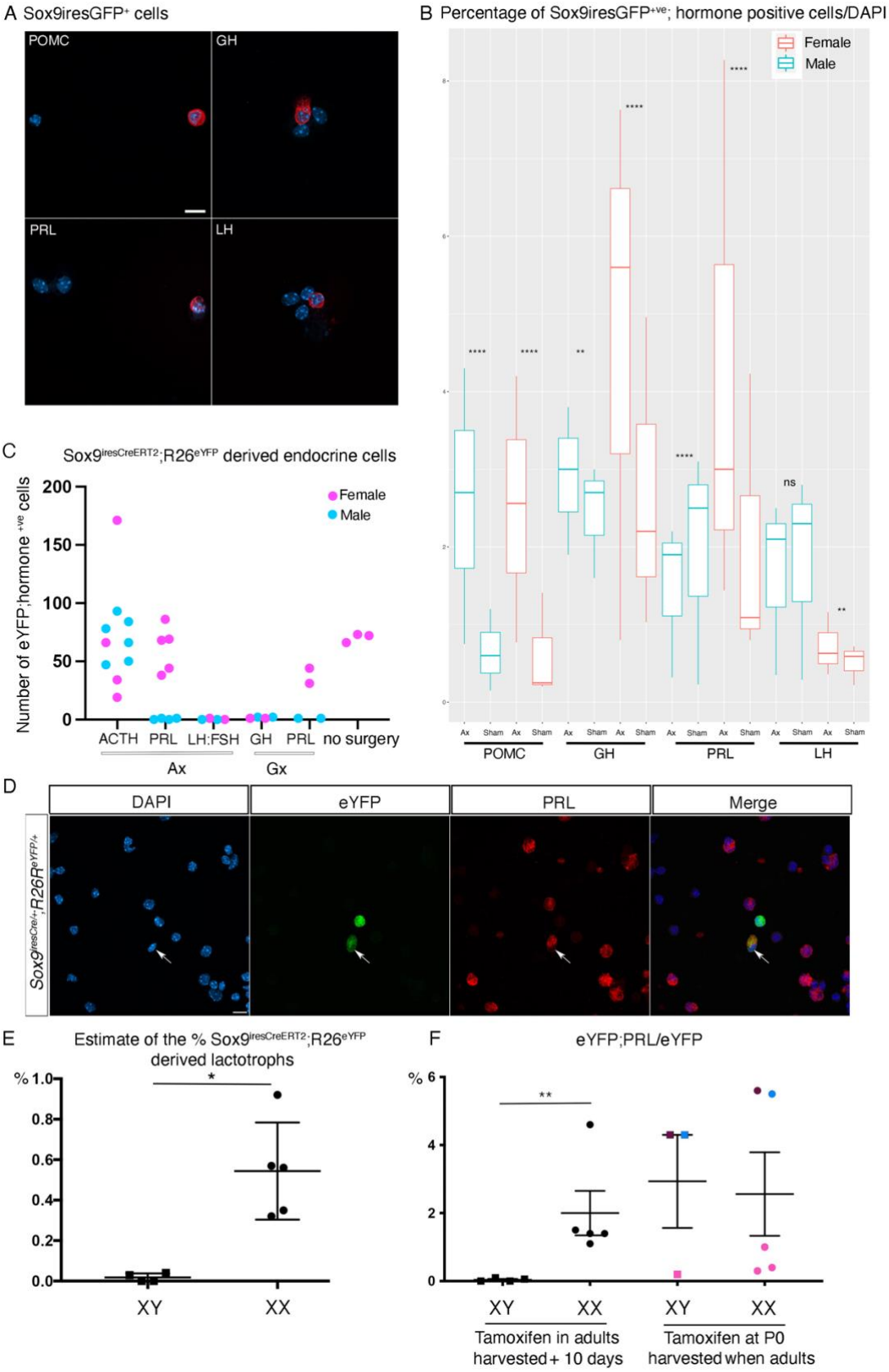

Figure 6: Analyses of scRNAseq predictions by short and long-term lineage tracing.

A) Immunofluorescence for hormonal markers on FACsorted Sox9iresGFP +ve cells from a female 4 days after Ax.

B) Percentages of FACSorted Sox9iresGFP +ve cells that are hormone +ve /DAPI. Cell counts were performed on plated cells (shown in A). Pituitaries were harvested 4 days after surgeries. Pairwise for proportion tests were performed to assess significance of differences between Ax and Sham (Sup. Table 2).

C) Numbers of hormone;eYFP double +ve cells counted in *Sox9*$^{iresCreERT2/+}$;*Rosa26*$^{ReYFP/+}$ pituitaries a week after surgeries or 10 days after tamoxifen treatment (no surgery). Counts were performed on comparable samples of whole pituitary sections. Corticotrophs are observed in both sexes after Ax, as previously reported. In contrast, significant numbers of lactotrophs are exclusively observed in females. LH;FSH cells have never been observed after gonadectomies (3) and were thus not quantified here.

D) Immunofluorescence for eYFP and PRL on dissociated non-sorted *Sox9*^{iresCreERT2};*Rosa26*^{ReYFP} female pituitary cells. A PRL;eYFP +ve cell is indicated (arrow).

C) Estimation of the percentage of lactotrophs differentiated from SCs. eYFP;PRL +ve cells from *Sox9*^{iresCreERT2};*Rosa26*^{ReYFP} dissociated pituitaries were counted 10 days after tamoxifen treatment. Numbers were corrected for induction efficiency, calculated in each animal as the percentage of SOX9;eYFP/SOX9 +ve cells present in the cleft. 0.6% of lactotrophs originate from SC 10 days after tamoxifen induction in females while we barely observed any in males (Mann-Whitney test performed on angular transformation of percentages, p=0.0159).

D) Percentage of PRL;eYFP/eYFP +ve cells 10 days after tamoxifen treatment in adults and after tamoxifen treatment in pups, harvested at 8 weeks of age (eYFP;PRL/eYFP in *Sox9*^{iresCreERT2};*Rosa26*^{ReYFP}). The proportion of SCs becoming lactotrophs is significantly higher in adult females compared to males. This sex bias disappears when tamoxifen is administered in pups (betareg test, p=0.00416). Despite injection of the same dose of tamoxifen in pups, there is a variability in the percentage of eYFP;Prl/eYFP +ve cells between litters (color coded). Scale bars represent 10 microns.

SCs and corticotrophs interact.

The selective maintenance of specific nascent SC progeny, while the rest are lost, suggests that survival is dependent on local cues in their microenvironment. In the context of Ax, the corticotrophs are a likely source of signals. We thus re-examined our transcriptomic datasets, screening for signalling pathways potentially activated in SCs by corticotrophs. We found that the receptor tyrosine kinase *Met* is selectively upregulated in SCs (Fig.7A, B) while its ligand *Hgf* is present both in corticotrophs and pericytes (Fig.7C, (28)), suggesting interactions between these cell types. Furthermore, *Met* is present at higher levels in SCs after Ax, when these become proliferative (Fig.7A). Because there are more corticotrophs after Ax, it is very likely that levels of HGF will increase too. Therefore, the MET pathway could mediate instructive or trophic actions of corticotrophs on SCs. The receptor and its ligand are both widely expressed in human pituitary adenomas (29).

Figure 7

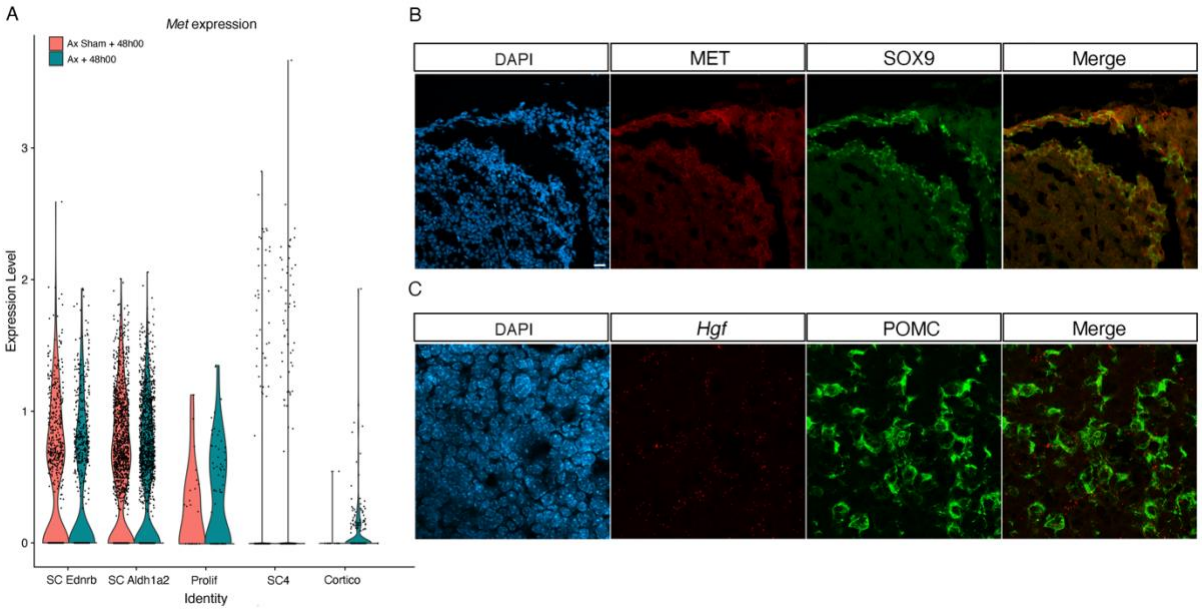

Figure 7: Expression of the receptor MET and its ligand *Hgf*.

A) Expression levels of *Met* on violin plots in clusters belonging to the corticotroph trajectory (Fig.5D). B) Immunofluorescence for MET and SOX9 showing the receptor is expressed in SCs. C) RNAscope and immunofluorescence for *Hgf* and POMC respectively showing that MET ligand is expressed in corticotrophs. *Hgf* is also predicted to be expressed in pericytes which could explain signal outside corticotrophs. Scale bar represents 20 microns in B and 10 microns in C.

DISCUSSION

While adult pituitary SCs appear superfluous for cell-turnover in the unchallenged animal, their regenerative potential can be stimulated, for example when the function of certain endocrine axes is compromised, such as when adrenals or gonads are ablated (3) (2, 5). Here we have characterized SC heterogeneity and the modalities of endocrine cell emergence, by examining Sox9iresGFP single cells. We observe that a small percentage of pituitary SCs differentiate in the unchallenged animal and that this proportion increases when SCs are mobilized. The paradigm we applied for SC mobilization, target organ ablation, is known to trigger a specific response in the pituitary: adrenal ablation results in increased ACTH while gonadectomy is associated with increased gonadotropins. However, although there was a significant induction of corticotroph cell fate acquisition shortly after ablation, we unexpectedly observed increased differentiation toward all AL endocrine cell types. Nevertheless, in the longer term, lineage tracing experiments show that it is exclusively the targeted endocrine cell type that is maintained in the SC progeny. Therefore, following differentiation, selective maintenance of specific nascent cells is an important process regulating pituitary SC endocrine cell output, and it seems likely that this is controlled by the SC microenvironment. Selective fitness of surviving cells in the embryo relies on access to particular trophic factors (30). In our Ax paradigm, the pituitary targets of the ablation, the corticotrophs, represent a likely source of signals. The

multiple roles of the MET-HGF signalling pathway in survival, proliferation, cell migration and promotion of regeneration (31) are certainly fitting with a trophic role of HGF secreting corticotrophs on MET positive SCs. Similarly, lactotrophs may be involved in the selective maintenance of nascent PRL cells emerging after tamoxifen treatment because prolactin secretion is increased by the SERM (32). In addition to the reliance on trophic factors, or maybe instead, it is likely that nascent cell maintenance involves integration into homotypic endocrine networks (33). This is reminiscent of what is known for nascent neurons that are often produced in excess and whose persistence relies on synaptic connections (34). Although focusing on SCs enabled us to uncover novel regulators and unexpected modalities of the regenerative response, our analyses point toward an important role for the microenvironment, and in our multi-organ system, peripheric factors which are predicted to modulate the regenerative response. The thyroid (*Thra*) and the androgen (*Ar*) hormone receptors appear active in differentiating SCs, suggesting that they can respond to peripheral signals, and maybe integrate this information to regulate pituitary plasticity, as recently proposed (35). Further investigations of both local and peripheral interactions are now required to better understand how the regenerative response is regulated.

Differential clustering of SOX9iresGFP +ve SCs, trajectory analyses and *in situ* validation of new markers revealed the activity of region-specific regulatory pathways. We speculate that RA may be involved in AL SC differentiation, as shown in the embryo (8). The downregulation of ALDH1a2 expression in IL SCs which do not differentiate (2, 36) provides an additional support to this hypothesis. In the trajectory analyses, the upstream expression pattern of *Ednrb* implies that the SCs lining the cleft are in a more immature state than those in the parenchyma, which fits with this epithelium constituting the primary pituitary SC niche. Among the 3 endothelin ligands, *Edn3* is the most abundantly expressed in the gland, more precisely in SCs and pericytes (28). This suggests that this pathway could function in an autocrine or paracrine way in cleft SCs, because these are not in close contact with capillaries (33), which would make an interaction with the latter unlikely. EDNRB signalling has been shown to regulate melanocyte SC regeneration (37) and we are currently investigating whether this role is conserved in pituitary SCs. The presence of RUNX, IFR and STAT regulons during cell differentiation is also of potential interest because of the roles of these factors in different SC contexts, and because they have been shown to interact (RUNX/STAT and IFR/STAT). STAT transcription factors are activated by different cytokines and growth factors, in particular IL6 whose role in the regenerative response of pituitary SCs was recently uncovered (38).

Our differentiation trajectories suggest the presence of a common root for all endocrine cell types, which only segregate as the terminal differentiation markers are upregulated in the nascent cells. This process is likely to be fast since cells still contain GFP expressed from *Sox9iresGFP*. It is now important to determine whether the same genes in this common root are associated with the different lineages and when specificity first appears. It is tempting to draw a parallel with embryonic pituitary progenitors, because these were similarly shown to all commit at the same stages (39). Interestingly, it was proposed that intrinsic factors and cell communication within the developing pituitary underlie specific endocrine cell fate acquisition, which, in a different context and with different modalities and outcomes, is what we hypothesize is happening in our model.

In conclusion, evaluation of single cell transcriptomic predictions with short and long-term lineage tracing experiments has proved a robust strategy revealing novel aspects of pituitary SC regenerative responses. In circumstances where an exceptional physiological need is

perceived, nascent cells of the appropriate type are maintained. Understanding how the new cells can survive will help us to understand how SC input is controlled in the pituitary, but this could also be relevant in other tissues where SC activity appears largely superfluous. Finally, it is notoriously difficult to obtain mature cell types *in vitro* for use in regenerative medicine. Therefore, identifying trophic factors for nascent cells, which may be all that can be obtained for transplantation, appears necessary.

Acknowledgements:

We are grateful for the support from present and past members of the Lovell-Badge lab. We are indebted to the Francis Crick institute platforms for their excellent support and expertise. We especially thank Jacek Mor from the Biological Research facility for taking excellent care of the animals, Donald Bell from the Advanced Light microscopy, Deborah Schneider-Luftman from Bioinformatics and Biostatistics and experts from the Advanced Sequencing and Histology platforms. We also thank Frederique Ruf-Zamojski and Zidong Zhang from the Icahn School of Medicine at Mount Sinai (New York) for sharing their expertise.
This work was supported by the Medical Research Council, U.K. (U117512772, U117562207 and U117570590) and the Francis Crick Institute which receives its core funding from Cancer Research UK (FC001107), the UK Medical Research Council (FC001107), and the Wellcome Trust (FC001107).

SUPPLEMENTARY FIGURE LEGENDS:

Sup. Figure 1: Co-localisation between SOX9 and ACTH after Ax.

Co-immunofluorescence for GFP, SOX9 and ACTH on sections of pituitaries harvested one week after Ax. Expression of Sox9iresGFP (A) and SOX9 (B) is observed in rare ACTH +ve cells (arrows) after Ax. The scale bar represents 10 µm for A and 5µm for B.

Sup. Figure 2: Expression of FS cells markers in SC and whole pituitary datasets.
A-C) UMAP for *S100b* (A), *Aldolase C* (B) and *Slc15a2* (C) in our Sox9iresGFP single cell dataset.
D-F) UMAP for *S100b* (D), *Sox2* (E) and *Aldolase C* (F) in a whole pituitary dataset (21).

Sup. Figure 3: Unchallenged/Challenged integrated analysis.
A) UMAP clustering and marker analysis for integrated datasets from sorted *Sox9*$^{iresGFP/+}$ cells from unchallenged, adrenalectomized, gonadectomized and both adrenalectomized and gonadectomized animals, 4 days after surgery.

B) Pairwise comparison for proportion test ('pairwise_prop_test' function [stats R package]) on stem cell clusters (circled on UMAP in A). The number of cells assigned to cluster 10 corresponding to proliferative cells (see *Top2a* expression in A) is significantly higher in activated stem cells (Sup. Table2).
C) Numbers and proportion of specific hormone +ve cells/all hormone +ve cells in each dataset. While we would expect the number of hormone +ve cells to increase after target organ ablation, as seen here, the fact that we select fewer GFP weak cells in unchallenged animals prevents us from comparing the proportion of hormone +ve cells in unchallenged and mobilized datasets and thus make this conclusion.

Sup. Figure 4: Analyses of marker expression on UMAP clustering on integrated analysis.
Markers of SC and hormone-secreting cell type are shown on the UMAP clustering for integrated datasets from GFP +ve cells sorted from *Sox9*$^{iresGFP/+}$ pituitaries from mice that were unchallenged, adrenalectomized and sham + 48 h, adrenalectomized + 4 days.

Sup. Figure 5: UMAP clustering for filtered integrated analysis split by dataset.
A) UMAP clustering for integrated datasets from sorted Sox9iresGFP +ve cells from unchallenged, adrenalectomized and sham + 48 h, adrenalectomized + 4 days split by dataset. SC clusters 3 and 4 mostly originate from datasets collected 48 hours after surgery. B) Expression of SC3 markers.

Sup. Figure 6: PCA clustering for filtered integrated analysis split by dataset.
SC4 cluster cells located in an intermediate position between SC and endocrine cells originate mostly from Ax+48h, which is consistent with mobilization and increased commitment toward differentiation.

Sup. Table1: Pathway analysis for clusters 0 and 2.
Gene markers for WT Cluster0 were used to determine enriched pathways with Metacore using a hypergeometric test. Pathways with an adjusted p value < 0.05 are shown in the table. Genes present in our dataset are highlighted in the top5 pathways.

Sup. Table2: Endocrine cell cluster numbers from Ax integrated dataset (Fig.5)

Sup. Table 3: Pairwise for proportion test results.

Sup. Table 4: Counting numbers for Fig. 5 and 6.

Sup. Table 5: Cell type signatures.

MATERIALS AND METHODS

Mice

All animal experiments carried out were approved under the UK Animals (Scientific Procedures) Act 1986 and under the project licences n. 80/2405 and PP8826065. *Sox9*$^{iresGFP/+}$ (*Sox9*^{tm1Haak}) (40), *Sox9*$^{iresCreERT2/+}$ (*Sox9*$^{tm1(cre/ERT2)Haak}$) (40), *Wnt1Cre* (*(no gene)*$^{tg(Wnt1-GAL4)11Rth}$) (41) and Rosa26$^{ReYFP/ReYFP}$ (*Gt(ROSA)26Sortm1(EYFP)Cos*) (42) mice were maintained on a C57Bl6 background.
For CreERT2 induction in *Sox9*$^{iresCreERT2/+}$;Rosa26$^{ReYFP/+}$ animals, tamoxifen was administered for 3 consecutive days at a concentration of 0.2mg/g body weight. For *Sox9*$^{iresCreERT2/+}$;Rosa26$^{ReYFP/+}$ pups induction, a single subcutaneous injection of tamoxifen (0.5mg/g body weight) was performed. Target organ ablations were performed as previously described (3).

Pituitary SC selection

The anterior lobe of freshly dissected pituitaries was minced and incubated for 15mn at 37ºC in 1mg/ml Papain (Sigma 10108014001), 10µg/ml DNAse I (Sigma 10104159001) and 10µg/ml Rock inhibitor (Abmole Bioscience M1817) in HBSS (Sigma H9394). pH was adjusted by addition of NaOH. The enzymatic solution was removed, and the cells were mechanically resuspended in HBSS supplemented with DNAse I and Rock inhibitor, as above. Cells were FACsorted for GFP using a large nozzle (100µm) and low pressure (20psi) for optimal cell survival. For immunofluorescence, sorted cells were plated on Superfrost slides for 90 min in a cell culture incubator, fixed 20 min on ice in 4% PFA and immediately processed.

Single cell sequencing

The concentration and viability of the single cell suspension was measured using Trypan Blue and the Eve automatic cell counter (unchallenged and target organ ablation d4 samples) or acridine orange and propidium iodide with the Luna-FX7 automatic cell counter (Ax and Sham control d2 samples). Up to 10,000 cells were loaded on Chromium Chip and partitioned in nanolitre scale droplets using the Chromium Controller and Chromium 10x 3 prime v2.0, Chromium Single Cell 3' Reagent Kits User Guide (v2 Chemistry) (unchallenged and target organ ablation d4 samples) or Next GEM Single Cell reagents (3 prime v3.1) (Ax and Sham control d2 samples). Within each droplet the cells were lysed, and the RNA was reverse transcribed. All of the resulting cDNA within a droplet shared the same cell barcode. Illumina compatible libraries were generated from the cDNA using Chromium Next GEM Single Cell library reagents in accordance with the manufacturer instructions (10x Genomics). Final libraries are quality checked using the Agilent TapeStation and sequenced using the Illumina HiSeq4000 or HiSeq2500, read configuration 26-8-0-98 (unchallenged and target organ ablation d4 samples) or NovaSeq 6000, read configuration 28-10-10-90.

Where expression of specific genes in the whole pituitary gland is referenced as ((28), we used this published dataset on the Loupe browser to examine expression of relevant markers.

Bioinformatic analyses

Alignment, Seurat analysis, integration and cluster annotation were performed using CellRanger and Seurat. Raw reads were initially processed by the Cell Ranger v.3.0.2 pipeline (43), which deconvolved reads to their cell of origin using the UMI tags, aligned these to the mm10 transcriptome (to which we added the eGFP sequence https://www.addgene.org/browse/sequence/305137/ to detect eGFP expressing cells) using STAR (v.2.5.1b) (44) and reported cell-specific gene expression count estimates. All subsequent analyses were performed in R v.3.6.0 (45) using the Seurat (v3) package (46). Genes were considered to be 'expressed' if the estimated (log10) count was at least 0.1. Primary filtering was then performed by removing from consideration cells expressing fewer than 50 genes and cells for which mitochondrial genes made up greater than 3 standard deviations from the mean of mitochondrial expressed genes. PCA decomposition was performed and, after consideration of the eigenvalue 'elbow-plots', the first 20 components were used to construct the UMAP plots per sample. Multiple samples, generated in this study and published (21), were integrated using 2000 variable genes and Seurat's CCA method. Cluster specific gene markers were identified using a Wilcoxon rank sum test and the top 20 genes ranked by logFC per cluster were used to generate a heatmap. Clusters were annotated using label tranfer methods within Seurat using the GSE120410 dataset (21). Clusters were further annotated using cell specific signatures (Sup. Table 5).
Cell trajectories were identified using the package 'Slingshot' (version 1.4.0) (22), using the undifferentiated cluster as a starting point and the PCA co-ordinates. Lineages were identified showing specific trajectories ending in specific differentiated cells. Differential expression of genes between samples were further investigated for the corticotroph lineage with a correlation metric against pseudotime, using the 'gam' package (version 1.20) (47). Heatmaps were made using the smoothed expression of differential genes, and the cells are ranked by increasing pseudotime.
In order to investigate transcription factor activity along pseudotime, the package SCENIC (25) was used. A list of 948 putative mouse regulatory binding sites found in promoter regions of expressed genes were used to identify shared regulatory networks. Regulon activity score per transcription factor was calculated using the AUCell function, where the enrichment of target genes was measured using the area under the curve of the target gene relative to the expression-based ranking of all genes. The top 200 regulons ranked by activity score were using to generate a binarized heatmap, where the cells were ranked by pseudotime.

Immunofluorescence and RNAscope.

Pituitaries were fixed after dissection by immersion in 4% PFA at 4ºC. Immunofluorescent stainings were performed on cryosections as described (48). The following primary antibodies were used: Goat anti-SOX2 (Biotechne, AF2018), rabbit anti-SOX9 (a gift from F. Poulat, IGH

Montpellier, France), rat anti-GFP (Nacalai Tesque 04404-84), rabbit anti-EDNRb (Abcam 117529), goat anti-MSX1 (R&D system AF5045), rabbit anti-ALDH1A2 (Abcam 75674, after antigen retrieval), rabbit anti-Claudin3 (Abcam ab15102), rat anti-PECAM (BD Pharmigen, 550274), rat anti-PDGFRβ (eBiosciences 14-1402-81), rabbit anti-Runx1 (Sigma, HPA004176), rabbit anti-IRF9 (Cell Signalling, D9I5H), goat anti-Met (R&D, AF 527) and hormone antibodies anti-LH, GH, ACTH and PRL from the National Hormone Peptide Program (A.F. Parlow, Torrance, USA). Slides were then incubated with Alexa Fluor secondary antibodies. Imaging of stained tissue sections was performed on a Leica SPE microscope while imaging of plated cells was done on an Olympus spinning disk microscope. RNAscope was performed on cryosections following the manufacturer's instructions using a *Hgf* probe (#456511).

Cell counts

Counts were performed blindly. For dissociated cell counts, slides stained by immunofluorescence were scanned; automated counts were then performed using QuPath (https://qupath.github.io/). For *Sox9*$^{iresCreERT2/+}$;Rosa26$^{ReYFP/+}$;hormone counting on sections, double +ve cells were manually identified and each imaged on a slide representing 1/5 of a pituitary. Images were then reviewed, and double +ve cells counted. All counting results are presented (Sup. Table 4).

Statistics

Comparisons of the percentages of Sox9;PDGFRβ (Fig.3) were performed after angular transformation using Mann-Whitney test on Prism. Pairwise for proportion test (Sup. Fig4B, Fig.5B, Fig.6B and Sup. Table 3) and betareg test (Fig.6E) were performed using the Stats R package.

Author contributions:

Conceptualization: KR, RLB
Methodology: KR
Bioinformatic analyses: PC
Investigation: KR, DS
Visualization: KR
Supervision: KR, RLB
Writing—original draft: KR
Writing—review & editing: KR, RLB

Competing interests:

Authors declare that they have no competing interests

Data and materials availability:

All data are available in the main text or the supplementary materials.
Codes are available on request. Datasets have been submitted (Awaiting confirmation of data deposited at GEO).

BIBLIOGRAPHY

1. A. Levy, Physiological implications of pituitary trophic activity. *J Endocrinol* **174**, 147-155 (2002).
2. D. Langlais, C. Couture, M. Kmita, J. Drouin, Adult pituitary cell maintenance: lineage-specific contribution of self-duplication. *Mol Endocrinol* **27**, 1103-1112 (2013).
3. K. Rizzoti, H. Akiyama, R. Lovell-Badge, Mobilized adult pituitary stem cells contribute to endocrine regeneration in response to physiological demand. *Cell Stem Cell* **13**, 419-432 (2013).
4. C. L. Andoniadou *et al.*, Sox2(+) stem/progenitor cells in the adult mouse pituitary support organ homeostasis and have tumor-inducing potential. *Cell Stem Cell* **13**, 433-445 (2013).
5. H. Roose *et al.*, Major depletion of SOX2(+) stem cells in the adult pituitary is not restored which does not affect hormonal cell homeostasis and remodelling. *Sci Rep* **7**, 16940 (2017).
6. Q. Fu *et al.*, The adult pituitary shows stem/progenitor cell activation in response to injury and is capable of regeneration. *Endocrinology* **153**, 3224-3235 (2012).
7. T. Fauquier, K. Rizzoti, M. Dattani, R. Lovell-Badge, I. C. Robinson, SOX2-expressing progenitor cells generate all of the major cell types in the adult mouse pituitary gland. *Proc Natl Acad Sci U S A* **105**, 2907-2912 (2008).
8. L. Y. M. Cheung, S. A. Camper, PROP1-Dependent Retinoic Acid Signaling Regulates Developmental Pituitary Morphogenesis and Hormone Expression. *Endocrinology* **161** (2020).
9. S. Yoshida *et al.*, Retinoic acid signalling is a candidate regulator of the expression of pituitary-specific transcription factor Prop1 in the developing rodent pituitary. *J Neuroendocrinol* **30**, e12570 (2018).
10. N. Nishimura *et al.*, Search for regulatory factors of the pituitary-specific transcription factor PROP1 gene. *J Reprod Dev* **62**, 93-102 (2016).
11. E. Laporte, A. Vennekens, H. Vankelecom, Pituitary Remodeling Throughout Life: Are Resident Stem Cells Involved? *Frontiers in endocrinology* **11**, 604519 (2020).
12. S. Yoshida *et al.*, Cell type-specific localization of Ephs pairing with ephrin-B2 in the rat postnatal pituitary gland. *Cell Tissue Res* **370**, 99-112 (2017).
13. M. I. Perez Millan, M. L. Brinkmeier, A. H. Mortensen, S. A. Camper, PROP1 triggers epithelial-mesenchymal transition-like process in pituitary stem cells. *Elife* **5** (2016).
14. P. R. Le Tissier, P. Mollard, Renewing an old interest: Pituitary folliculostellate cells. *J Neuroendocrinol* 10.1111/jne.13053, e13053 (2021).
15. L. O'Hara, H. C. Christian, N. Jeffery, P. Le Tissier, L. B. Smith, Characterisation of a mural cell network in the murine pituitary gland. *J Neuroendocrinol* **32**, e12903 (2020).
16. K. Fujiwara *et al.*, Aldolase C is a novel molecular marker for folliculo-stellate cells in rodent pituitary. *Cell Tissue Res* **381**, 273-284 (2020).

17. W. Allaerts, H. Vankelecom, History and perspectives of pituitary folliculo-stellate cell research. *Eur J Endocrinol* **153**, 1-12 (2005).
18. S. W. Davis *et al.*, beta-catenin is required in the neural crest and mesencephalon for pituitary gland organogenesis. *BMC Dev Biol* **16**, 16 (2016).
19. H. C. Etchevers, C. Vincent, N. M. Le Douarin, G. F. Couly, The cephalic neural crest provides pericytes and smooth muscle cells to all blood vessels of the face and forebrain. *Development* **128**, 1059-1068 (2001).
20. L. A. Nolan, A. Levy, A population of non-luteinising hormone/non-adrenocorticotrophic hormone-positive cells in the male rat anterior pituitary responds mitotically to both gonadectomy and adrenalectomy. *J Neuroendocrinol* **18**, 655-661 (2006).
21. L. Y. M. Cheung *et al.*, Single-Cell RNA Sequencing Reveals Novel Markers of Male Pituitary Stem Cells and Hormone-Producing Cell Types. *Endocrinology* **159**, 3910-3924 (2018).
22. K. Street *et al.*, Slingshot: cell lineage and pseudotime inference for single-cell transcriptomics. *BMC Genomics* **19**, 477 (2018).
23. J. E. Welcker *et al.*, Insm1 controls development of pituitary endocrine cells and requires a SNAG domain for function and for recruitment of histone-modifying factors. *Development* **140**, 4947-4958 (2013).
24. J. Drouin, The corticotroph cells from early development to tumorigenesis. *J Neuroendocrinol* **34**, e13147 (2022).
25. S. Aibar *et al.*, SCENIC: single-cell regulatory network inference and clustering. *Nat Methods* **14**, 1083-1086 (2017).
26. K. M. Osorio, K. C. Lilja, T. Tumbar, Runx1 modulates adult hair follicle stem cell emergence and maintenance from distinct embryonic skin compartments. *J Cell Biol* **193**, 235-250 (2011).
27. C. M. Horvath, G. R. Stark, I. M. Kerr, J. E. Darnell, Jr., Interactions between STAT and non-STAT proteins in the interferon-stimulated gene factor 3 transcription complex. *Mol Cell Biol* **16**, 6957-6964 (1996).
28. A. Mayran *et al.*, Pioneer and nonpioneer factor cooperation drives lineage specific chromatin opening. *Nature communications* **10**, 3807 (2019).
29. X. Z. Hou *et al.*, Expression of hepatocyte growth factor and its receptor c-Met in human pituitary adenomas. *Neuro Oncol* **12**, 799-803 (2010).
30. Y. Wang *et al.*, A cell fitness selection model for neuronal survival during development. *Nature communications* **10**, 4137 (2019).
31. L. Trusolino, A. Bertotti, P. M. Comoglio, MET signalling: principles and functions in development, organ regeneration and cancer. *Nat Rev Mol Cell Biol* **11**, 834-848 (2010).
32. D. Gonzalez *et al.*, Luteinizing hormone secretion elicited in a ligand-independent activation of progesterone receptor manner at pituitary level in the rat: differential effect of two selective estrogen receptor modulators. *Neurosci Lett* **289**, 111-114 (2000).
33. P. Mollard, D. J. Hodson, C. Lafont, K. Rizzoti, J. Drouin, A tridimensional view of pituitary development and function. *Trends Endocrinol Metab* **23**, 261-269 (2012).
34. W. Kelsch, C. W. Lin, C. P. Mosley, C. Lois, A critical period for activity-dependent synaptic development during olfactory bulb adult neurogenesis. *J Neurosci* **29**, 11852-11858 (2009).

35. P. R. Le Tissier, J. F. Murray, P. Mollard, A New Perspective on Regulation of Pituitary Plasticity: The Network of SOX2-Positive Cells May Coordinate Responses to Challenge. *Endocrinology* **163** (2022).
36. V. Moncho-Amor *et al.*, SOX2 is required independently in both stem and differentiated cells for pituitary tumorigenesis in p27-null mice. *Proc Natl Acad Sci U S A* **118** (2021).
37. M. Takeo *et al.*, EdnrB Governs Regenerative Response of Melanocyte Stem Cells by Crosstalk with Wnt Signaling. *Cell reports* **15**, 1291-1302 (2016).
38. A. Vennekens *et al.*, Interleukin-6 is an activator of pituitary stem cells upon local damage, a competence quenched in the aging gland. *Proc Natl Acad Sci U S A* **118** (2021).
39. S. W. Davis, A. H. Mortensen, S. A. Camper, Birthdating studies reshape models for pituitary gland cell specification. *Developmental biology* **352**, 215-227 (2011).
40. K. Furuyama *et al.*, Continuous cell supply from a Sox9-expressing progenitor zone in adult liver, exocrine pancreas and intestine. *Nat Genet* **43**, 34-41 (2010).
41. P. S. Danielian, D. Muccino, D. H. Rowitch, S. K. Michael, A. P. McMahon, Modification of gene activity in mouse embryos in utero by a tamoxifen-inducible form of Cre recombinase. *Curr Biol* **8**, 1323-1326 (1998).
42. S. Srinivas *et al.*, Cre reporter strains produced by targeted insertion of EYFP and ECFP into the ROSA26 locus. *BMC Dev Biol* **1**, 4 (2001).
43. G. X. Zheng *et al.*, Massively parallel digital transcriptional profiling of single cells. *Nature communications* **8**, 14049 (2017).
44. A. Dobin *et al.*, STAR: ultrafast universal RNA-seq aligner. *Bioinformatics* **29**, 15-21 (2013).
45. R. C. Team, R: A language and environment for statistical computing. *R Foundation for Statistical Computing, Vienna, Austria.* (2019).
46. T. Stuart *et al.*, Comprehensive Integration of Single-Cell Data. *Cell* **177**, 1888-1902 e1821 (2019).
47. T. Hastie, gam: Generalized Additive Models. . *R package version 1.20* (2020).
48. K. Rizzoti *et al.*, SOX3 is required during the formation of the hypothalamo-pituitary axis. *Nat Genet* **36**, 247-255 (2004).

Sup. Fig.1

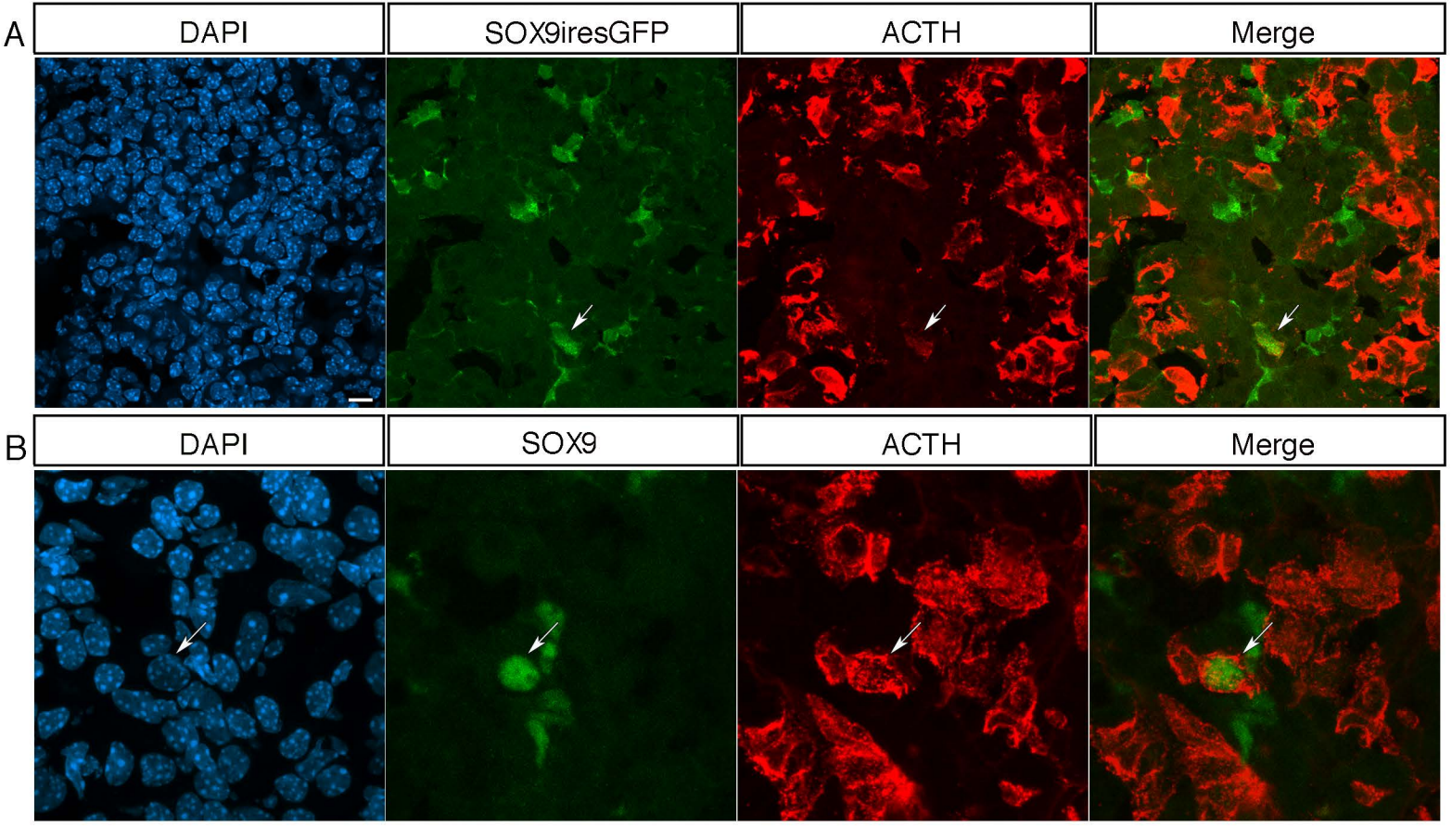

Sup. Fig.2

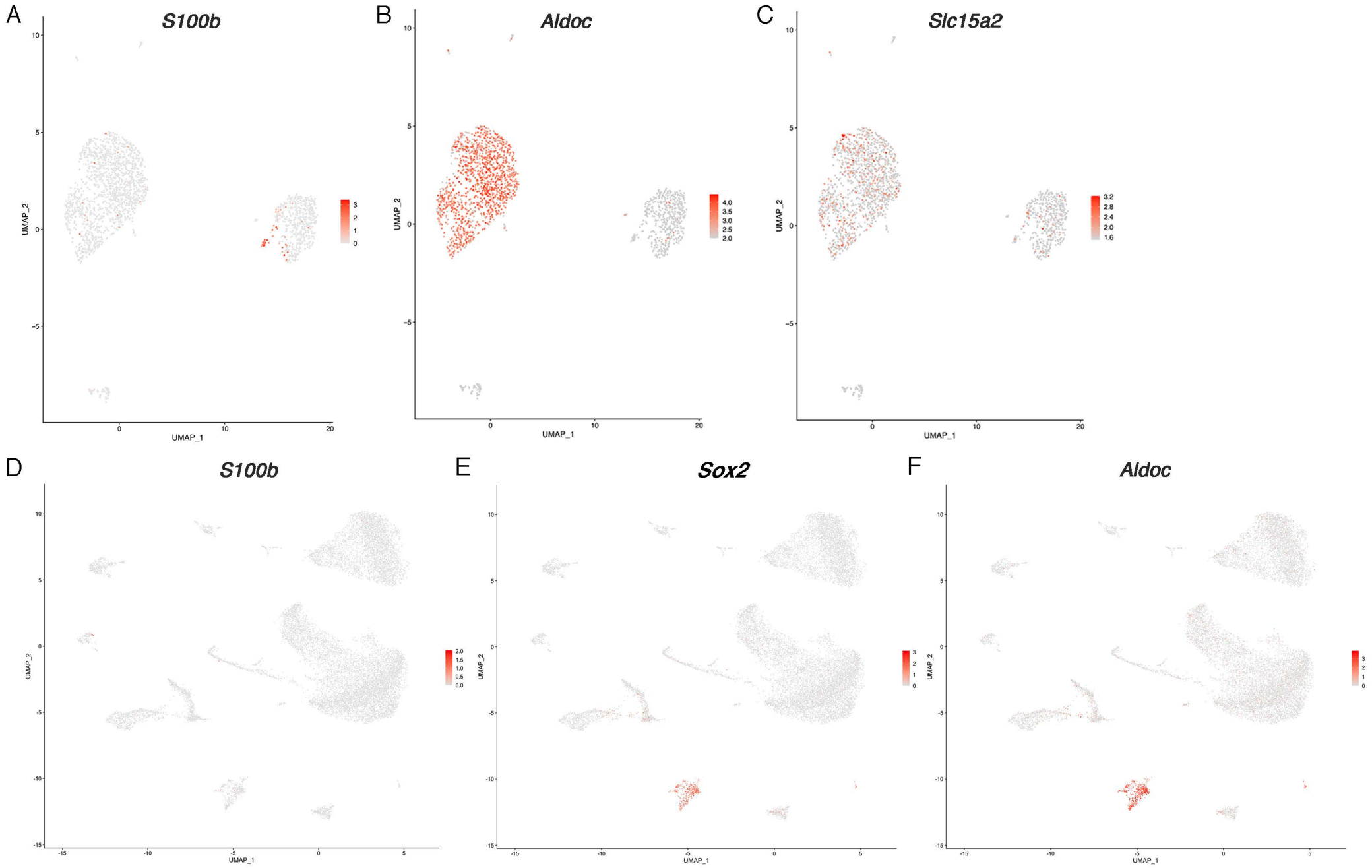

Sup. Fig.3

A

Sox2
Sox9
Ednrb
Aldh1a2
Pou1f1
Prl
Tshb
Gh
Tbx19
rna_Pax7
Pomc
Nr5a1
Lhb
Fshb
Pdgfrb
Top2a
UMAP_1
UMAP_2

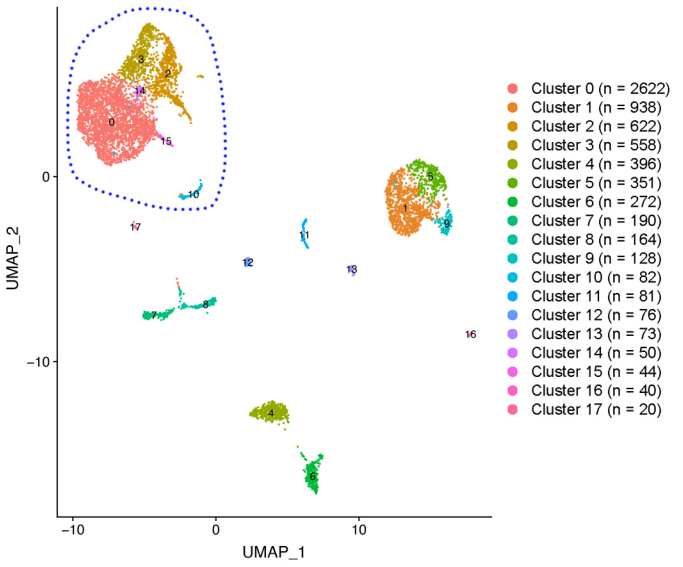
Cluster 0 (n = 2622)
Cluster 1 (n = 938)
Cluster 2 (n = 622)
Cluster 3 (n = 558)
Cluster 4 (n = 396)
Cluster 5 (n = 351)
Cluster 6 (n = 272)
Cluster 7 (n = 190)
Cluster 8 (n = 164)
Cluster 9 (n = 128)
Cluster 10 (n = 82)
Cluster 11 (n = 81)
Cluster 12 (n = 76)
Cluster 13 (n = 73)
Cluster 14 (n = 50)
Cluster 15 (n = 44)
Cluster 16 (n = 40)
Cluster 17 (n = 20)
UMAP_1
UMAP_2

B

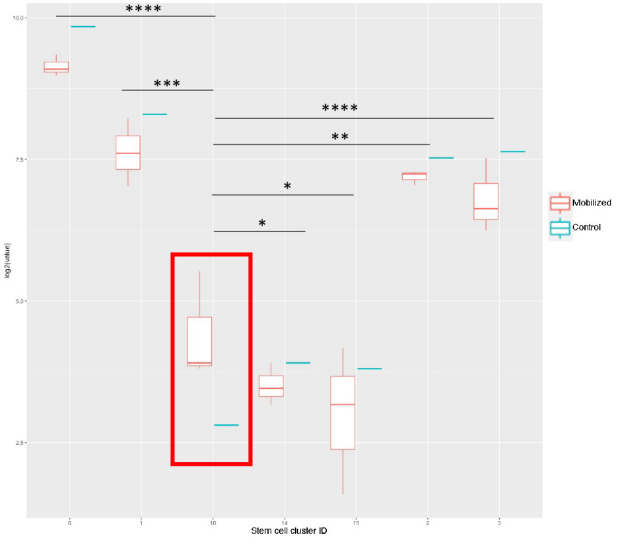
****
***
****
**
*
*
Mobilized
Control
Stem cell cluster ID

C

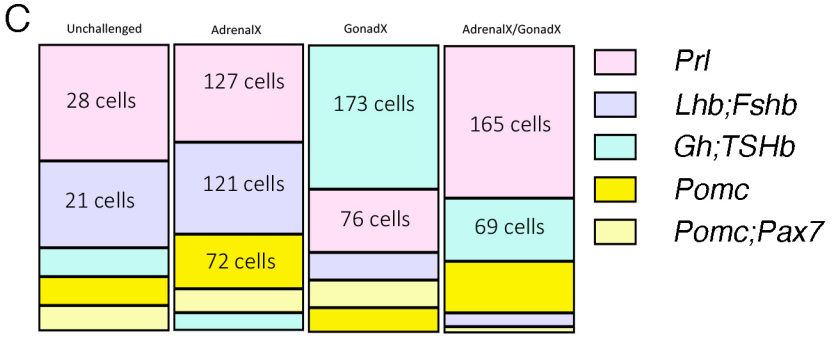
Unchallenged
AdrenalX
GonadX
AdrenalX/GonadX
28 cells
21 cells
127 cells
121 cells
72 cells
173 cells
76 cells
165 cells
69 cells
Prl
Lhb;Fshb
Gh;TSHb
Pomc
Pomc;Pax7

Sup. Fig.4

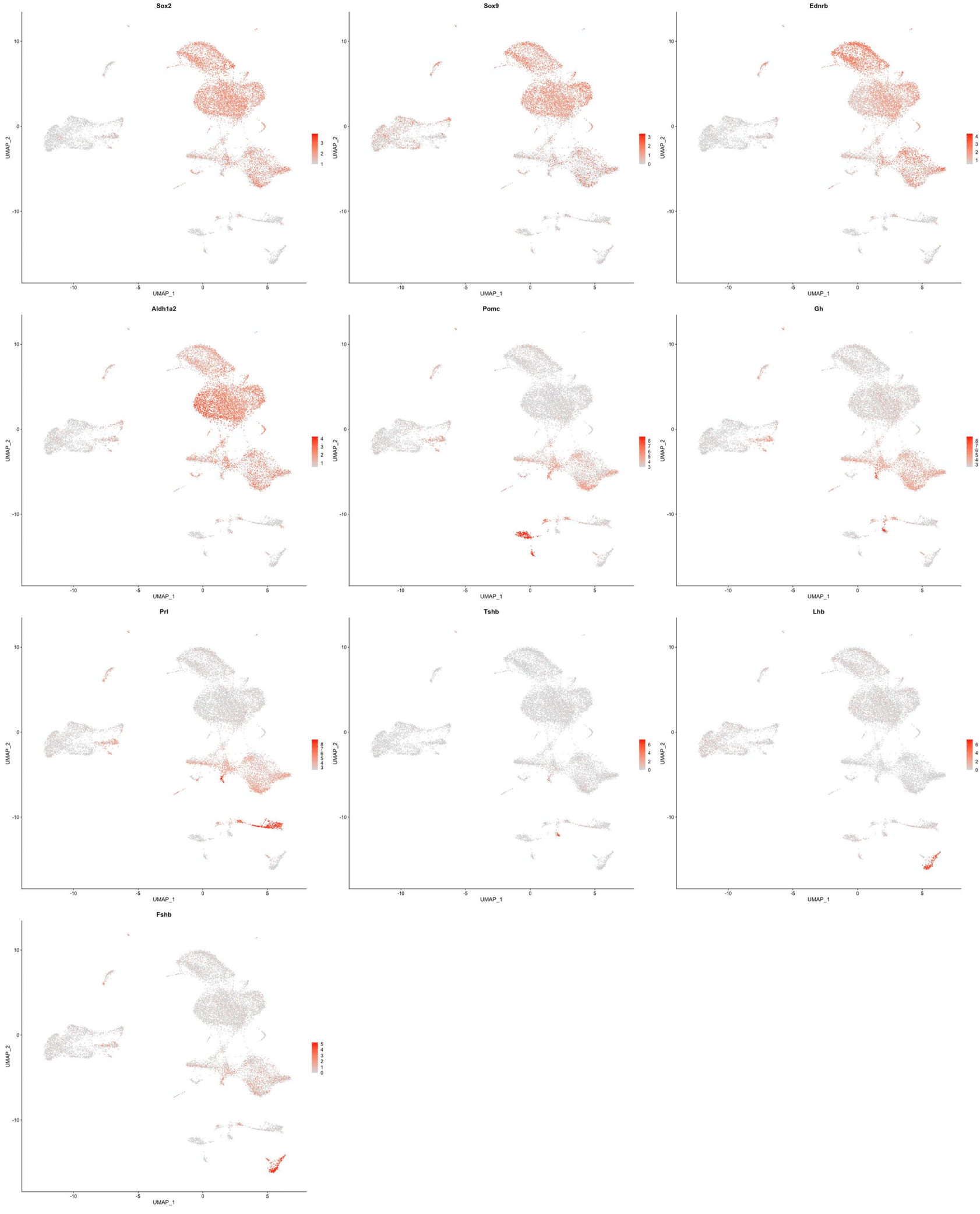
Sox2
Sox9
Ednrb
Aldh1a2
Pomc
Gh
Prl
Tshb
Lhb
Fshb
UMAP_1
UMAP_2

Sup. Fig.5

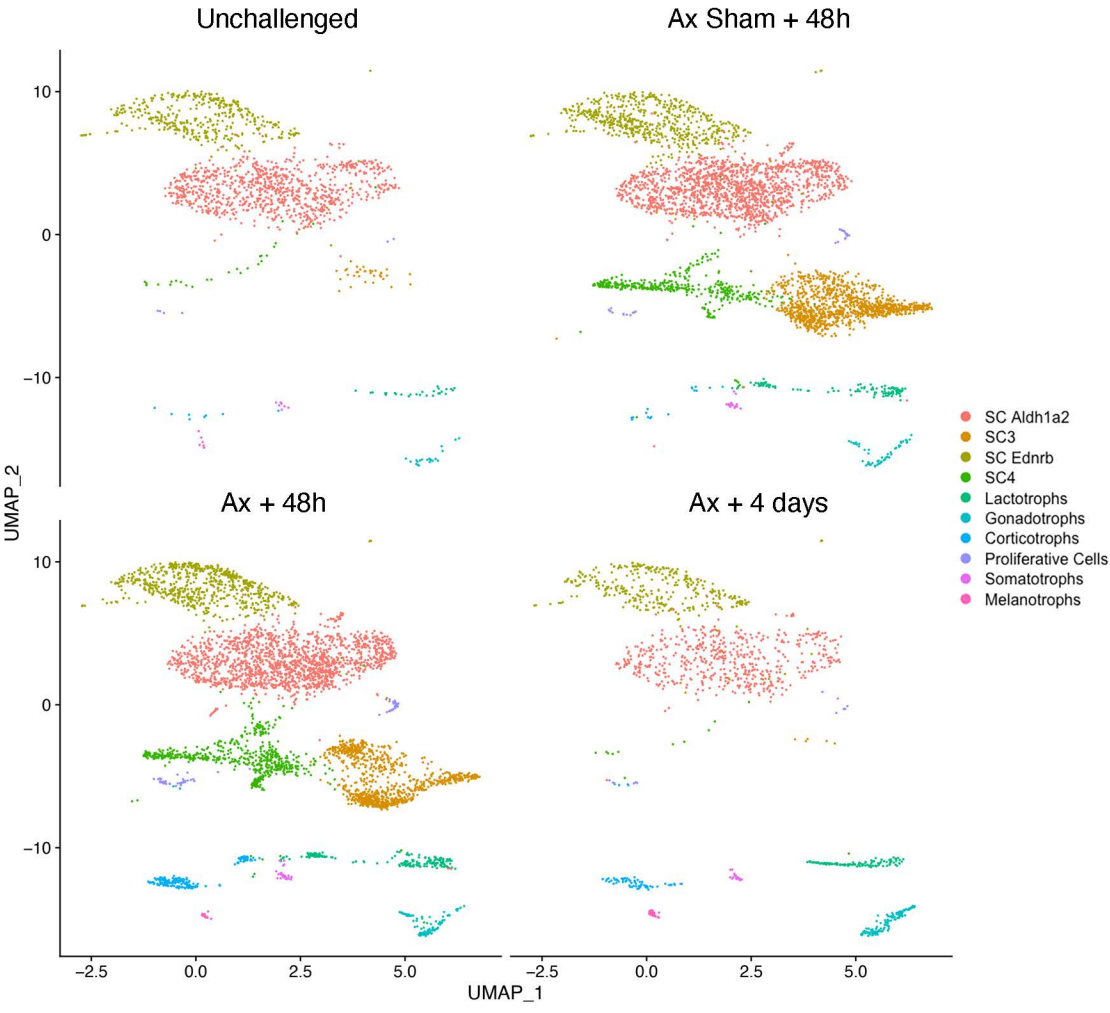
Unchallenged
Ax Sham + 48h
Ax + 48h
Ax + 4 days
UMAP_2
UMAP_1
10
0
−10
−2.5
0.0
2.5
5.0
SC Aldh1a2
SC3
SC Ednrb
SC4
Lactotrophs
Gonadotrophs
Corticotrophs
Proliferative Cells
Somatotrophs
Melanotrophs

Sup. Fig.6

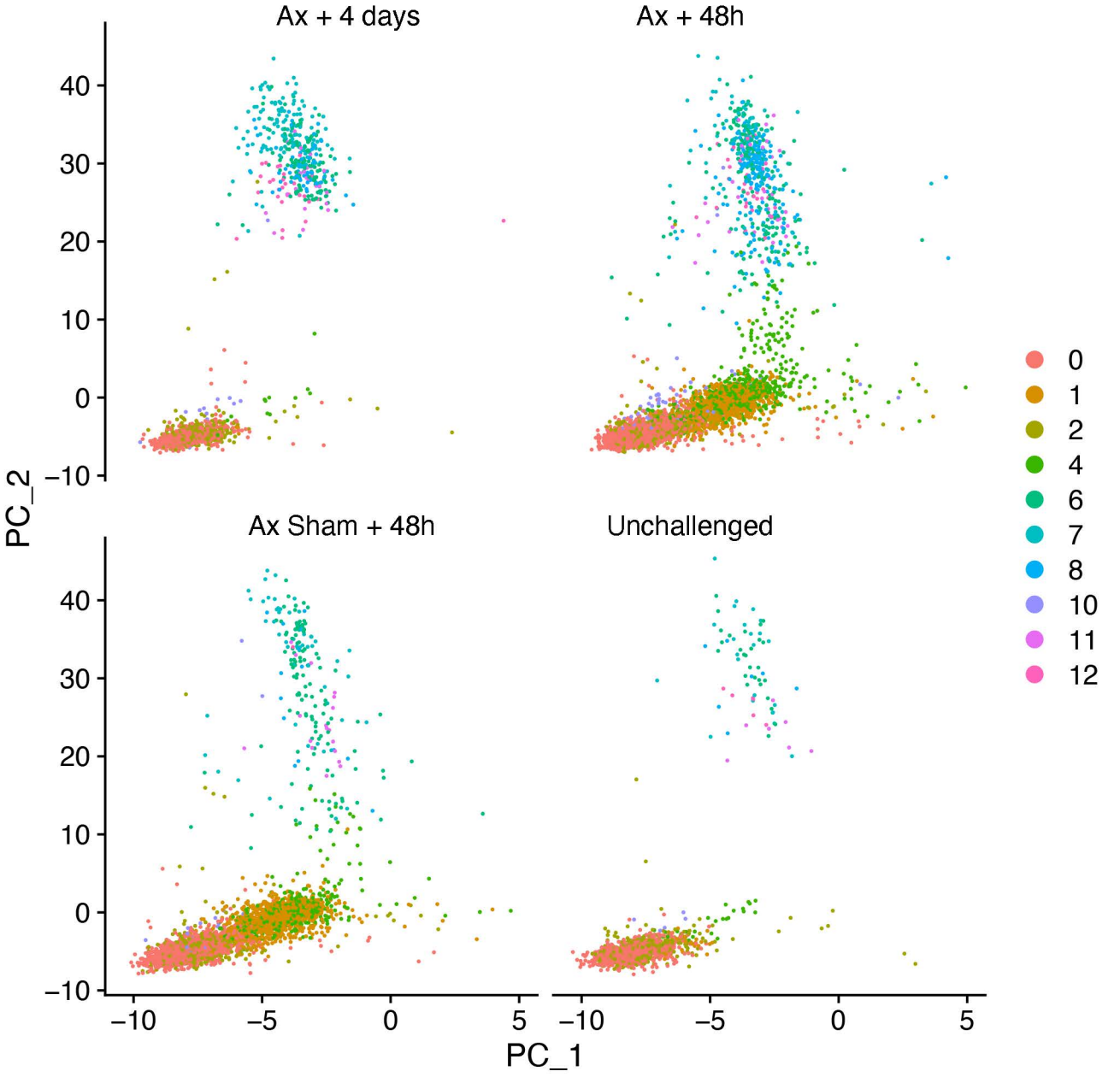
Ax + 4 days
Ax + 48h
Ax Sham + 48h
Unchallenged
PC_2
PC_1
40
30
20
10
0
−10
−10
−5
0
5
0
1
2
4
6
7
8
10
11
12

Supplementary Table 1

Enrichment analysis report

Enrichment by Pathway Maps

					NT Cluster-0, operator			
#	Maps	Total	pValue	Min FDR	p-value	FDR	In Data	Network Objects From Active Data
1	Gamma-secretase proteolytic targets	80	2.041E-11	2.445E-08	2.041E-11	2.445E-08	18	NOTCH2 (2ICD), LRP1B, alpha/APPs, LRP1B (ICD), N-cadherin, NOTCH2 receptor, APP-C99, N-cadherin (CTF1), APP-CIB (CTF), N-cadherin (CTF2), Ephrin-B2, LRP1B (CTF), Ephrin-B2 (CTF2), APP-C59 (AICD), Amyloid beta 40, NOTCH2(NEXT), Amyloid beta 42, APP
2	Development, Extraembryonic differentiation of embryonic stem cells	35	6.983E-07	4.183E-04	6.983E-07	4.183E-04	9	ID2, ID4, HEY1, SOX2, ID1, MAP2, NCAM1, PAX6, CD9
3	Nuclear receptors in action of bilirubin	63	2.603E-06	7.638E-04	2.603E-06	7.638E-04	11	FRAT1, Thioredoxin, Amyloid beta, P2X2, IPP-1, NR2A, WNT, NR2, p38 MAPK, Frizzled, c-Jun
4	Development, NOTCH1 signaling in the nervous system	89	2.634E-06	7.638E-04	2.634E-06	7.638E-04	13	NOTCH2 (2ICD), ID4, HEY1, SOX2, NOTCH2 receptor, Aquaporin 4, HES1, Adrogin, Cyclin D1, NFIA, PAX6, NOTCH2(NEXT), Clusterin
5	Development, NOTCH signaling in myelinogenesis and oligodendrocyte	77	3.188E-06	7.638E-04	3.188E-06	7.638E-04	12	SIX2, NOTCH2 (2ICD), IRF6, HEY1, NOTCH2 receptor, HES1, Islet-1, HEY2, Ephrin-B2, Activin beta A, Connexin 43, NRARP
6	Inhibition of oligodendrocyte precursor cells differentiation by Wnt signaling in multiple sclerosis	25	6.731E-06	1.220E-03	6.731E-06	1.220E-03	7	FZD1, ID2, WNT9A, FZD7, WNT, Frizzled, FZD4
7	Gamma-Secretase regulation of neuronal cell development and function	57	7.131E-06	1.220E-03	7.131E-06	1.220E-03	10	N-cadherin, Amyloid beta, APP-C99, Fe65, N-cadherin (CTF1), N-cadherin (CTF2), APP-C59 (AICD), Amyloid beta 40, betaAPPs, APP
8	Gamma-secretase regulation of gastrointestinal epithelial cell development	28	1.533E-05	2.266E-03	1.533E-05	2.266E-03	7	NOTCH2 (2ICD) , HEY1, NOTCH2 receptor, HES1, HEY2, PAX6, NOTCH2(NEXT)
9	Role of Gli1 transcriptome in multiple myeloma	40	2.198E-05	2.925E-03	2.198E-05	2.925E-03	8	Nxf8, N-cadherin, NOTCH2 receptor, ID1, HES1, Cyclin D1, NCAM1, Histone H3
10	Inhibition of Ephrin receptors in colorectal cancer	30	2.500E-05	2.995E-03	2.500E-05	2.995E-03	7	Ephrin-B2, Ephrin-B, WNT, Ephrin-B receptors, Ephrin-A receptors, Frizzled, Ephrin-B receptor 1
11	Deregulation of canonical WNT signaling in major depressive disorder	31	3.146E-05	3.193E-03	3.146E-05	3.193E-03	7	FRAT1, FZD3, WNT, Cyclin D1, FZD9, MAP-1B, Frizzled
12	Transcription targets of Androgen receptor involved in Prostate Cancer	42	3.198E-05	3.193E-03	3.198E-05	3.193E-03	8	Androgen receptor, N-cadherin, ERBB, Cyclin D1, Prosaposin, VIL2 (ezrin), Clusterin, APP
13	Cell adhesion, Gap junctions	22	3.713E-05	3.357E-03	3.713E-05	3.357E-03	6	Tubulin beta, Actin cytoskeletal, Actin, Calmodulin, Connexin 43, VIL2 (ezrin)
14	Stem cells, Notch signaling in medulloblastoma stem cells	32	3.923E-05	3.357E-03	3.923E-05	3.357E-03	7	NOTCH2 (2ICD), HEY1, NOTCH2 receptor, HES1, HEY2, Cyclin D1, NOTCH2(NEXT)
15	Role of activation of WNT signaling in the progression of lung cancer	77	1.055E-04	8.437E-03	1.055E-04	8.437E-03	10	FZD1, FZD3, WNT9A, FZD7, WNT, Cyclin D1, p38 MAPK, FZD9, CD147, Frizzled
16	Signal transduction, NOTCH signaling in tissue homeostasis	81	1.624E-04	1.195E-03	1.624E-04	1.195E-03	10	NOTCH2 (2ICD) , Androgen receptor , HEY1, NOTCH2 receptor, HES1, HEY2, Ephrin-B2, c-Jun, OAT, CYP19
17	WNT signaling in HCC	40	1.763E-04	1.195E-03	1.763E-04	1.195E-03	7	FZD3, Ep-CAM, FZD7, WNT, Cyclin D1, GLNA, Frizzled
18	Immune response, Induction of the antigen presentation machinery by IFN-gamma	53	1.795E-04	1.195E-03	1.795E-04	1.195E-03	8	H2-Aa, H2-Eb1, HLA-E, MHC class II, HLA-F, HLAC, CD74, HLA-DMA
19	Immune response, Antigen presentation by MHC class II	118	2.422E-04	1.527E-03	2.422E-04	1.527E-03	12	MHC class II alpha chain, HSP90, Kinesin light chain, MHC class II beta chain, Dynein 1, cytoplasmic, intermediate chains, HLA-DM, MHC class II, p38 MAPK, HSP90 beta, CLEC10A, Legumain, CD74
20	Glutathione metabolism	71	2.809E-04	1.683E-03	2.809E-04	1.683E-03	9	GCL cat, GSTM1, GSTA3, GSTM2, GSTM5, MGST, GGTL3, GSTM1 (rodent), GSTT1
21	Oxidative stress, Role of Sirtuins and FOXO-3 alpha in activation of antioxidant defense system	60	4.308E-04	2.458E-03	4.308E-04	2.458E-03	8	GCL cat, SCPX, Thioredoxin, PRDX1, TXNRD1, GSTM5, UCP2, PRDX5
22	Development, TGF-beta dependent induction of EMT via SMAD4	35	5.787E-04	3.126E-03	5.787E-04	3.126E-03	6	ID2, HEY1, N-cadherin, TGF-beta 2, TGF-beta, MKL1
23	Transcription, HIF-1 targets	95	6.001E-04	3.126E-03	6.001E-04	3.126E-03	10	ID2, SOX2, TGF-beta 2, PHHA1, ALDOC, DEC2, ENO1, REDD1, PKM2, GPI
24	Beta catenin dependent transcription regulation in colorectal cancer	36	6.769E-04	3.379E-03	6.769E-04	3.379E-03	6	ID2, Cyclin D1, NRCAM, LAMC2, LAMC2 (80kDa), LAMC2 (300kDa)
25	Development, NOTCH signaling activation	82	8.250E-04	3.953E-03	8.250E-04	3.953E-03	9	NOTCH2 (2ICD), HEY1, NOTCH2 receptor, HES1, HEY2, BAF60c, HDAC3, MS1, NOTCH2(NEXT)
26	Canonical Notch signaling pathway in colorectal cancer	52	9.256E-04	4.123E-03	9.256E-04	4.123E-03	7	NOTCH2 (2ICD) , NOTCH2 receptor , HES1, WNT, Cyclin D1, NOTCH2(NEXT), HES6
27	Cell adhesion, Endothelial cell contacts by junctional mechanisms	26	9.753E-04	4.123E-03	9.753E-04	4.123E-03	5	N-cadherin, Actin cytoskeletal, Cingulin, Alpha-catenin, Connexin 43
28	Cell adhesion, Classical cadherin-mediated cell adhesion	26	9.753E-04	4.123E-03	9.753E-04	4.123E-03	5	N-cadherin, Actin cytoskeletal, F-Actin cytoskeleton, Alpha-catenin, F-Actin
29	Cell cycle progression in Prostate Cancer	39	1.050E-03	4.123E-03	1.050E-03	4.123E-03	6	Androgen receptor, WNT, Cyclin D1, p38 MAPK, Frizzled, c-Jun
30	Activation of Notch signaling in breast cancer	39	1.050E-03	4.123E-03	1.050E-03	4.123E-03	6	HEY1, HES1, p38 MAPK, c-Jun, MS1, Presenilin
31	Transcription, Negative regulation of HIF1A function	69	1.111E-03	4.123E-03	1.111E-03	4.123E-03	8	HSP90, PRDX2, SIP1, DEC2, HSP90 beta, KLF2, HIF-prolyl hydroxylase, EGLN2
32	NRF2 regulation of oxidative stress response	54	1.163E-03	4.123E-03	1.163E-03	4.123E-03	7	GCL cat, GSTA3, Thioredoxin, PRDX1, TXNRD1, Actin cytoskeletal, CRIM1
33	Stem cells, NOTCH1-induced self-renewal of medulloblastoma stem cells	40	1.205E-03	4.123E-03	1.205E-03	4.123E-03	6	HEY1, SOX2, ID1, HES1, HEY2, Cyclin D1
34	Gamma-secretase regulation of notch signaling	40	1.205E-03	4.123E-03	1.205E-03	4.123E-03	6	NOTCH2 (2ICD), HEY1, NOTCH2 receptor, HES1, Cyclin D1, NOTCH2(NEXT)
35	Stem cells, Response to hypoxia in medulloblastoma stem cells	40	1.205E-03	4.123E-03	1.205E-03	4.123E-03	6	HEY1, ID1, HES1, HEY2, Cyclin D1, HIF-prolyl hydroxylase
36	DNA damage, ATM activation by DNA damage	71	1.341E-03	4.343E-03	1.341E-03	4.343E-03	8	HSP90, HMGA1A, p38, PP2A regulatory, HSP90 beta, Histone H2B, IHPK2, Histone H3
37	Development, Positive regulation of STAT3 (Hippo) pathway and negative regulation of YAP/TAZ fate	71	1.341E-03	4.343E-03	1.341E-03	4.343E-03	8	EBP50, Angiomotin (AMOT), Actin cytoskeletal, MALS-3, Alpha-catenin, Alpha-1 catenin, G-protein alpha-s, 14-3-3
38	G-protein signaling, Rac2 regulation pathway	17	1.453E-03	4.580E-03	1.453E-03	4.580E-03	4	Androgen receptor, Actin cytoplasmic 2, Calmyrin, F-Actin
39	Ribosome metabolism	74	1.756E-03	5.333E-03	1.756E-03	5.333E-03	8	MTND1, NDUFA4, MT-ND5, MTND4, MTND2, NDUFC2, DAP13, MTND3
40	Notch signaling in breast cancer	58	1.781E-03	5.333E-03	1.781E-03	5.333E-03	7	NOTCH2 (2ICD) , HEY1, NOTCH2 receptor, HES1, HEY2, Cyclin D1, NOTCH2(NEXT)
41	Androgen receptor activation and downstream signaling in Prostate cancer	110	1.865E-03	5.450E-03	1.865E-03	5.450E-03	10	Androgen receptor, N-cadherin, ERBB, SGK1, Cyclin D1, Prosaposin, FGF1, VIL2 (ezrin), Clusterin, APP
42	Development, Transcription factors in specification of hepatocytic lineage	30	1.912E-03	5.454E-03	1.912E-03	5.454E-03	5	Activin A, Activin B, Cyclin D1, Activin, GGTL3
43	Apoptotic mitotic and cytotoxic induced hair cell death	112	2.134E-03	5.746E-03	2.134E-03	5.746E-03	10	NKX3, AP-1, p38 MAPK, HDAC3, Histone H2B, Cathepsin D, CX3CL1, c-Jun, Histone H3, LMO4
44	Role of inhibition of WNT signaling in the progression of lung cancer	31	2.224E-03	5.746E-03	2.224E-03	5.746E-03	5	N-cadherin, CD82, FZD9, Frizzled, c-Jun
45	Development, Endocrinal neuronal morphogenesis	31	2.224E-03	5.746E-03	2.224E-03	5.746E-03	5	FZD1, HES1, WNT, Pitx2, Frizzled
46	Development, Negative regulation of WNT/Beta-catenin signaling at the receptor level	45	2.253E-03	5.746E-03	2.253E-03	5.746E-03	6	LRP4, Amyloid beta, WNT, Frizzled, FZD-6, Syndecans
47	Inhibition of WNT7A-dependent non-canonical pathway in colorectal cancer	19	2.255E-03	5.746E-03	2.255E-03	5.746E-03	4	Cyclin D1, Calmodulin, CRIM1, c-Jun
48	Neurophysiological process, ACM1, ACM2 and ACM3 signaling in the brain	78	2.461E-03	6.141E-03	2.461E-03	6.141E-03	8	alphaAPPs, TRPM3, APP-CIB (CTF), Calmodulin, betaAPPs, CACNB3, APP
49	Inhibition of neurotrophin in multiple sclerosis, role of cell-cell and ECM-cell interactions	47	2.820E-03	6.894E-03	2.820E-03	6.894E-03	6	CD99, Actin cytoskeletal, CD82, NCAM1, Connexin 43, CD9
50	Role of Shh and Notch in SCLC	33	2.955E-03	6.946E-03	2.955E-03	6.946E-03	5	NOTCH2 (2ICD), NOTCH2 receptor, HES1, ALLA1, NOTCH2(NEXT)

Supplementary Table 1

Enrichment analysis report

Enrichment by Pathway Maps

#	Maps	Total	pValue	Min FDR	WT Cluster 2 genes p-value	FDR	In Data	Network Objects from Active Data
1	Cytoskeleton remodeling_Keratin filaments	38	5.894E-09	4.697E-06	5.894E-09	4.697E-06	8	Keratin 19, Keratin 17, Tubulin alpha, Keratin 8, Keratin 8/18, Vimentin, Keratin 18, Keratin 7
2	Cytoskeleton remodeling_Regulation of actin cytoskeleton organization by the kinase effectors of Rho-s	58	3.015E-07	1.202E-04	3.015E-07	1.202E-04	8	Rac3, MLCP (cat), Rhotv_Spectrin, MRLC, Rac1-related, WRCH-1, Cdc42 subfamily
3	Cell adhesion_Desmosomes	19	1.935E-06	5.139E-04	1.935E-06	5.139E-04	5	Keratin 17, Keratin 8/18, Vimentin, Keratin 18, Plakoglobin
4	Cell adhesion_Tight junctions	44	1.038E-05	1.891E-03	1.038E-05	1.891E-03	6	PKC-zeta, Tubulin alpha, Occludin, MRLC, CRB3, ZO-3
5	Mechanisms of resistance to EGFR inhibitors in lung cancer	45	1.186E-05	1.891E-03	1.186E-05	1.891E-03	6	HSP90, Claudin-7, Ep-CAM, Vimentin, Claudin-4, TACSTD2 (TROP2)
6	Canonical Notch signaling pathway in colorectal cancer	52	2.775E-05	3.687E-03	2.775E-05	3.687E-03	6	KLF4, NOTCH1 (NICD), NOTCH1 (NEXT), KLF5, NOTCH1 receptor, NOTCH1 precursor
7	Oxidative stress_ROS-induced cellular signaling	108	3.412E-05	3.885E-03	3.412E-05	3.885E-03	8	HSP27, NOTCH1 (NICD), TXNIP (VDUP1), FTH1, NFKBIA, Pin1, DLC1 (Dynein LC8a), PKC
8	Possible regulation of HSF-1/ chaperone pathway in Huntington's disease	21	8.687E-05	8.655E-03	8.687E-05	8.655E-03	4	HSP90, HSP27, PLA2, HSP90 alpha
9	Signal transduction_Relaxin family peptides signaling via RXFP1 and RXFP2 receptors	70	1.508E-04	1.335E-02	1.508E-04	1.335E-02	6	NOTCH1 (NICD), PKC-zeta, NOTCH1 (NEXT), EDNRB, NFKBIA, I-kB
10	Cytoskeleton remodeling_Regulation of actin cytoskeleton nucleation and polymerization by Rho GTPases	46	1.776E-04	1.415E-02	1.776E-04	1.415E-02	5	Rac3, mDIA2(DIAPH3), Rac1-related, DRF, Cdc42 subfamily
11	Cell adhesion_Endothelial cell contacts by junctional mechanisms	26	2.075E-04	1.503E-02	2.075E-04	1.503E-02	4	Occludin, Vimentin, Claudin-3, Plakoglobin
12	Glucocorticoids-mediated inhibition of pro-constrictory and pro-inflammatory signaling in airway smoo	48	2.403E-04	1.596E-02	2.403E-04	1.596E-02	5	MLCP (cat), PLA2, NFKBIA, MRLC, MKP-1
13	Notch signaling in oligodendrocyte precursor cell differentiation in multiple sclerosis	29	3.209E-04	1.968E-02	3.209E-04	1.968E-02	4	NOTCH1 (NICD), NOTCH1 (NEXT), SOX10, NOTCH1 receptor
14	Development_Auditory hair cell differentiation in embryogenesis	32	4.176E-04	2.378E-02	4.176E-04	2.378E-02	4	NOTCH1 (NICD), NOTCH1 (NEXT), NOTCH1 receptor, NOTCH1 precursor
15	Skeletal muscle atrophy in COPD	57	4.901E-04	2.604E-02	4.901E-04	2.604E-02	5	NFKBIA, I-kB, Vimentin, 14-3-3, JunD
16	Notch signaling in breast cancer	58	5.314E-04	2.620E-02	5.314E-04	2.620E-02	5	NOTCH1 (NICD), NOTCH1 (NEXT), Pin1, NOTCH1 receptor, NOTCH1 precursor
17	Development_NOTCH signaling in the nervous system	88	5.589E-04	2.620E-02	5.589E-04	2.620E-02	6	NOTCH1 (NICD), PKC-zeta, NOTCH1 (NEXT), SOX10, NOTCH1 receptor, Clusterin
18	Development_WNT and Notch signaling in early cardiac myogenesis	35	6.706E-04	2.969E-02	6.706E-04	2.969E-02	4	NOTCH1 (NICD), SFRP5, NOTCH1 (NEXT), NOTCH1 receptor
19	Immune response_IL-4 signaling pathway	94	7.471E-04	2.995E-02	7.471E-04	2.995E-02	6	AP-1, PKC-zeta, Tubulin alpha, NFKBIA, PKC, JunD
20	Cytoskeleton remodeling_Substance P-mediated membrane blebbing	18	7.515E-04	2.995E-02	7.515E-04	2.995E-02	3	MLCP (cat), Tubulin alpha, MRLC
21	Stem cells_CD30 signaling in transformed embryonic stem cells	18	1.077E-03	4.087E-02	1.077E-03	4.087E-02	3	KLF4, I-kB, TRAF1
22	Development_NOTCH-induced EMT	19	1.268E-03	4.593E-02	1.268E-03	4.593E-02	3	NOTCH1 (NICD), NOTCH1 (NEXT), NOTCH1 receptor
23	Signal transduction_Non-neuronal ACh1, AC-M1 and AC-M3 signaling	74	1.613E-03	5.588E-02	1.613E-03	5.588E-02	5	MLCP (cat), PKC-zeta, MRLC2, MRLC, PKC
24	Role of DNA methylation in progression of multiple myeloma	45	1.746E-03	5.797E-02	1.746E-03	5.797E-02	4	AP-1, SFRP5, DKK3, NOTCH1 receptor
25	Signal transduction_Angiotensin II/AGTR1 signaling via Notch, Beta-catenin and NF-kB pathways	78	2.037E-03	6.495E-02	2.037E-03	6.495E-02	5	NOTCH1 (NICD), NOTCH1 (NEXT), I-kB, NOTCH1 receptor, PKC
26	Development_NOTCH signaling activation	92	2.538E-03	7.781E-02	2.538E-03	7.781E-02	5	NOTCH1 (NICD), PKC-zeta, NOTCH1 (NEXT), NOTCH1 receptor, NOTCH1 precursor
27	HSP70 and HSP40-dependent folding in Huntington's disease	29	2.861E-03	8.446E-02	2.861E-03	8.446E-02	3	HSP90, HSP27, HSP90 alpha
28	Signal transduction_Additional pathways of NF-kB activation (in the cytoplasm)	52	2.981E-03	8.485E-02	2.981E-03	8.485E-02	4	PKC-zeta, NFKBIA, Pin1, I-kB
29	Gamma-secretase regulation of gastrointestinal epithelial cell development	28	3.974E-03	1.056E-01	3.974E-03	1.056E-01	3	NOTCH1 (NICD), NOTCH1 (NEXT), NOTCH1 receptor
30	Rho-dependent regulation of normal and asthmatic smooth muscle contraction	28	3.974E-03	1.056E-01	3.974E-03	1.056E-01	3	MLCP (cat), MRLC, PKC
31	Development_VEGF signaling via VEGFR2 - generic cascades	93	4.372E-03	1.070E-01	4.372E-03	1.070E-01	5	HSP90, HSP27, I-kB, PKC, PLA2G5
32	Cigarette smoke-mediated regulation of NRF2 antioxidant pathway in airway epithelial cells	29	4.396E-03	1.070E-01	4.396E-03	1.070E-01	3	GSTO1, TALDO, DJ-1
33	Aberrant production of IL-2 and IL-17 in SLE T cells	58	4.430E-03	1.070E-01	4.430E-03	1.070E-01	4	NOTCH1 (NICD), AP-1, I-kB, NOTCH1 precursor
34	Gamma-secretase regulation of angiogenesis	36	4.843E-03	1.103E-01	4.843E-03	1.103E-01	3	NOTCH1 (NICD), NOTCH1 (NEXT), NOTCH1 receptor
35	Signal transduction_Additional pathways of NF-kB activation (in the nucleus)	36	4.843E-03	1.103E-01	4.843E-03	1.103E-01	3	PKC-zeta, NFKBIA, I-kB
36	Role of inhibition of WNT signaling in the progression of lung cancer	31	5.317E-03	1.177E-01	5.317E-03	1.177E-01	3	Keratin 8, Vimentin, Keratin 18
37	Stem cells_Notch signaling in medulloblastoma stem cells	32	5.818E-03	1.253E-01	5.818E-03	1.253E-01	3	NOTCH1 (NICD), NOTCH1 (NEXT), NOTCH1 receptor
38	Role of SHH and Notch in SCLC	33	6.347E-03	1.292E-01	6.347E-03	1.292E-01	3	NOTCH1 (NICD), NOTCH1 (NEXT), NOTCH1 receptor
39	LRRK2 in neurons in Parkinson's disease	33	6.347E-03	1.292E-01	6.347E-03	1.292E-01	3	HSP90, PKC-zeta, 14-3-3
40	Development_NOTCH1 signaling in the epidermis	65	6.645E-03	1.292E-01	6.645E-03	1.292E-01	4	NOTCH1 (NICD), NOTCH1 (NEXT), I-kB, NOTCH1 receptor
41	Signal transduction_PDGF signaling via MAPK cascades	65	6.645E-03	1.292E-01	6.645E-03	1.292E-01	4	HSP27, KLF4, AP-1, JunD
42	Development_Epigenetic and transcriptional regulation of oligodendrocyte precursor cell differentiation	34	6.903E-03	1.310E-01	6.903E-03	1.310E-01	3	NOTCH1 (NICD), SOX10, NOTCH1 receptor
43	Development_TGF-beta-dependent induction of EMT via SMAD's	35	7.488E-03	1.356E-01	7.488E-03	1.356E-01	3	NOTCH1 (NICD), Occludin, Vimentin
44	Immune response_Lipoxins and Resolvin E1 inhibitory action on neutrophil functions	35	7.488E-03	1.356E-01	7.488E-03	1.356E-01	3	PKC-zeta, NFKBIA, I-kB
45	HBV signaling via protein kinases leading to HCC	36	8.100E-03	1.435E-01	8.100E-03	1.435E-01	3	AP-1, Pin1, PKC
46	Immune response_Plasmin signaling	70	8.612E-03	1.492E-01	8.612E-03	1.492E-01	4	Annexin II, NFKBIA, PKC, JunD
47	TNF-alpha-induced inflammatory signaling in normal and asthmatic airway epithelium	38	9.412E-03	1.576E-01	9.412E-03	1.576E-01	3	NFKBIA, IFN14(TNFRSF12A), I-kB
48	Signal transduction_Calcium-mediated signaling	72	9.494E-03	1.576E-01	9.494E-03	1.576E-01	4	MLCP (cat), I-kB, PKC, 14-3-3
49	Activation of Notch signaling in breast cancer	39	1.011E-02	1.630E-01	1.011E-02	1.630E-01	3	KLF4, NOTCH1 (NICD), NOTCH1 precursor
50	Gamma-secretase regulation of osteogenesis	40	1.084E-02	1.630E-01	1.084E-02	1.630E-01	3	NOTCH1 (NICD), NOTCH1 (NEXT), NOTCH1 receptor

Supplementary Table 2

		Number of cells				
ID	Cluster ID	AX+ 4days	AX+ 48h00	AXSham	WT	
SC Aldh1a2	0	541	1606	1492	910	
SC3	1	7	941	1068	36	
SC Ednrb	2	334	685	593	409	
Dcn	3	427	403	493	484	
SC4	4	12	603	387	27	
Dcn/vasc	5	7	212	237	24	
Lacto	6	127	198	120	28	
Gonado	7	136	94	56	22	
Cortico	8	69	199	14	7	
Dcn/vasc	9	22	72	86	21	
Prolif	10	13	69	26	6	
Somato	11	24	37	18	7	
Melano	12	31	33	1	6	
Dcn/vasc	13	0	25	13	5	
Dcn/vasc	14	15	18	4	1	
		1765	5195	4608	1993	
Endo cells total		387	561	209	70	
%endo/total (endo=Clusters 6,7,8,14 and15)		22	11	4.5	3.5	
% lacto/endo		32	35	57	40	
% cortico/endo		18	35	7	3	
		AX+ 4days	AX+ 48h00	AXSham	WT	
%cortico/total		4	3.8	0.3	0.3	
%lacto/total		7.2	3.8	2.6	1.4	
% somato/total		1.3	0.7	0.4	0.3	
% gonado/total		7.7	1.8	1.2	1.1	

Supplementary Table 3

Showing 1 to 6 of 6 entries, 5 total columns						
Pairwise for proportion test (Fig.5B)						
	group1	**group2**	**p**	**p.adj**	**p.adj.signif**	
1	SC Aldh1a2	SC3	5.35E-04	1.02E-02	*	
2	SC3	SC Ednrb	1.82E-04	4.18E-03	**	
3	SC Aldh1a2	SC4	7.50E-07	2.03E-05	****	
4	SC3	SC4	5.55E-13	1.72E-11	****	
5	SC Ednrb	SC4	5.76E-04	1.04E-02	*	
6	SC Aldh1a2	Prolif	9.91E-05	2.38E-03	**	
7	SC3	Prolif	1.50E-06	3.74E-05	****	
8	SC Ednrb	Prolif	4.83E-04	1.01E-02	*	
9	SC Aldh1a2	Lacto	4.88E-04	1.01E-02	*	
10	SC3	Lacto	4.36E-07	1.22E-05	****	
11	SC3	Gonado	2.54E-04	5.59E-03	**	
12	SC Aldh1a2	Cortico	1.02E-31	3.56E-30	****	
13	SC3	Cortico	7.30E-38	2.63E-36	****	
14	SC Ednrb	Cortico	1.46E-27	4.97E-26	****	
15	SC4	Cortico	1.39E-19	4.60E-18	****	
16	Prolif	Cortico	1.36E-06	3.54E-05	****	
17	Lacto	Cortico	1.23E-15	3.95E-14	****	
18	Gonado	Cortico	6.99E-13	2.10E-11	****	
19	Cortico	Somato	3.40E-07	9.87E-06	****	
Showing 1 to 19 of 19 entries, 5 total columns						
Pairwise for proportion test (Fig.6B)						
	n	Statistic	df	p.value	adj.p.value	p.signif
POMC.in.ma	27347	174.098914	1	9.42E-40	2.51E-39	****
PRL.in.males	35836	15.302442	1	9.16E-05	1.47E-04	****
LH.in.males	35836	1.803625	1	1.79E-01	1.79E-01	ns
GH.in.males	31383	10.574053	1	1.15E-03	1.31E-03	**
POMC.in.fem	60958	404.277391	1	6.45E-90	5.16E-89	****
PRL.in.femal	62693	235.560711	1	3.65E-53	1.46E-52	****
LH.in.female	62693	10.638566	1	1.11E-03	1.31E-03	**
GH.in.female	57634	165.802853	1	6.11E-38	1.22E-37	****

Supplementary Table 4

Sox9;PDGFRb counts were exclusively performed in the parenchyma (cleft excluded) on triple immunofluorescence (GFP for Sox9iresGFP, Sox9 to insure nucleus was that of a Sox9 postive cell and PDGFRb)				
Manual coutings				
Animal	Sex	Age	Sox9iresGFP;Sox9	Sox9iresGFP;Sox9;PDGFRb
1	XY	6m-old	387	39
2	XY	6 m-old	265	19
3	XY	6 m-old	291	24
4	XY	8 m-old	616	39
1	XX	2 m-old	331	7
2	XX	4 m-old	734	10
3	XX	8 m-old	739	9
4	XX	4 m-old	807	5
Cell countings after lineage tracing using Wnt1Cre on triple immunofluorescence (GFP for Wnt1Cre;R26 eYFP, Sox9 and PDGFRb)				
Manual countings				
Animal	Sex	Age	Sox9;PDGFRb	Sox9;PDGFRb;eYFP
1	XY	6w-old	49	36
2	XY	6w-old	55	43
3	XY	6w-old	35	26
4	XY	6w-old	33	25
5	XY	6w-old	55	43
6	XY	6w-old	66	62
1	XX	6w-old	21	9
2	XX	6w-old	17	9

Figure 3 countings

Supplementary Table 4

Dissociated Sox9iresGFP pituitaries were FACSorted and plated 4 days after surgery. Immunofluorescent stainings performed as follow: GH and POMC separately, LH and PRL as a double-immuno.

Automated countings

Experiment	positive	DAPI	sum	protein	Sex
Ax	20	2617	2637	POMC	Male
Ax	162	5878	6040	POMC	Male
Ax	221	4945	5166	POMC	Male
ShAx	5	3255	3260	POMC	Male
ShAx	25	4183	4208	POMC	Male
ShAx	72	5964	6036	POMC	Male
Ax	33	4224	4257	POMC	Female
Ax	276	10518	10794	POMC	Female
Ax	479	10744	11223	POMC	Female
ShAx	17	6684	6701	POMC	Female
ShAx	251	17558	17809	POMC	Female
ShAx	20	10154	10174	POMC	Female
Ax	9	2836	2845	PRL	Male
Ax	142	7180	7322	PRL	Male
Ax	165	7214	7379	PRL	Male
ShAx	8	3439	3447	PRL	Male
ShAx	119	4631	4750	PRL	Male
ShAx	312	9781	10093	PRL	Male
Ax	48	3331	3379	PRL	Female
Ax	1093	12121	13214	PRL	Female
Ax	415	13231	13646	PRL	Female
ShAx	50	4512	4562	PRL	Female
ShAx	764	17302	18066	PRL	Female
ShAx	83	9743	9826	PRL	Female
Ax	10	2835	2845	LH	Male
Ax	156	7166	7322	LH	Male
Ax	183	7196	7379	LH	Male
ShAx	10	3437	3447	LH	Male
ShAx	110	4640	4750	LH	Male
ShAx	282	9811	10093	LH	Male
Ax	12	3367	3379	LH	Female
Ax	153	13061	13214	LH	Female
Ax	87	13559	13646	LH	Female
ShAx	10	4552	4562	LH	Female
ShAx	130	17936	18066	LH	Female
ShAx	58	9768	9826	LH	Female
Ax	53	2721	2774	GH	Male
Ax	196	6195	6391	GH	Male
Ax	291	7313	7604	GH	Male
ShAx	46	2823	2869	GH	Male
ShAx	178	6409	6587	GH	Male
ShAx	155	5003	5158	GH	Male
Ax	19	2331	2350	GH	Female
Ax	923	11164	12087	GH	Female
Ax	571	9587	10158	GH	Female
ShAx	36	3430	3466	GH	Female
ShAx	1034	19796	20830	GH	Female
ShAx	194	8549	8743	GH	Female

Figure 6B countings

Supplementary Table 4

A week after surgeries Sox9iresCreERT2;R26eYFP pituitaries were processed for immunofluorescence on sections								
Countings were performed manually on sections								
Animal	Age	Sex	Surgery	ACTH;eYFP				
1	<=7 w-old	XX	Ax	66				
2	<=7 w-old	XX	Ax	34				
3	<=7 w-old	XX	Ax	171				
4	<=7 w-old	XX	Ax	19				
1	<=7 w-old	XY	Ax	84				
2	<=7 w-old	XY	Ax	93				
3	<=7 w-old	XY	Ax	66				
4	<=7 w-old	XY	Ax	47				
5	<=7 w-old	XY	Ax	50				
6	<=7 w-old	XY	Ax	78				
Animal	Age	Sex	Surgery	PRL;eYFP				
1	<=7 w-old	XX	Ax	38				
2	<=7 w-old	XX	Ax	68				
3	<=7 w-old	XX	Ax	44				
4	<=7 w-old	XX	Ax	69				
5	<=7 w-old	XX	Ax	86				
1	<=7 w-old	XY	Ax	1				
2	<=7 w-old	XY	Ax	1				
3	<=7 w-old	XY	Ax	0				
4	<=7 w-old	XY	XY	0				
Animal	Age	Sex	Surgery	LH or FSH;eYFP				
1	<=7 w-old	XX	Ax	0				
2	<=7 w-old	XX	Ax	1				
1	<=7 w-old	XY	Ax	0				
2	<=7 w-old	XY	Ax	0				
Animal	Age	Sex	Surgery	GH;eYFP				
1	<=7 w-old	XX	Gx	1				
2	<=7 w-old	XX	Gx	1				
1	<=7 w-old	XY	Gx	2				
2	<=7 w-old	XY	Gx	2				
Animal	Age	Sex	Surgery	Prl;eYFP				
1	<=7 w-old	XX	Gx	31				
2	<=7 w-old	XX	Gx	44				
1	<=7 w-old	XY	Gx	1				
2	<=7 w-old	XY	Gx	1				
Animal	Age	Sex	Surgery	Prl;eYFP				
1	<=7 w-old	XX	None	66				
2	<=7 w-old	XX	None	73				
3	<=7 w-old	XX	None	72				

Supplementary Table 4

Figure 6C countings

Supplementary Table 4

Cre induction efficiency quantification. On the day of dissociation, the central part of the pituitary was kept to quantify the percentage of recombination on cleft-lining SOX9 positive cells.

Manual countings

Animal	Sex	Age	SOX9	SOX9;eYFP	%induction
1	XY	8 w-old	1076	142	13
2	XY	8 w-old	651	100	15.3
3	XY	8 w-old	972	141	14.5
4	XY	8 w-old	1285	223	17.3
1	XX	8 w-old	527	51	9.6
2	XX	8 w-old	990	140	14
3	XX	8 w-old	789	133	16.9
4	XX	8 w-old	1331	204	15.3
5	XX	8 w-old	1260	209	16.6

Figure 6E countings

Supplementary Table 4

Automated Prl;eYFP countings in adult dissociated AL Sox9CreERT2;ReYFP 10 days after induction							
Animal	Sex	Age	DAPI	Prl	eYFP	Prl;eYFP	%induction
1	XY	8 w-old	53433	8774	906	0	13
2	XY	8 w-old	118487	21203	1507	1	15.3
3	XY	8 w-old	93587	16065	932	1	14.5
4	XY	8 w-old	124853	21223	1373	0	17.3
1	XX	8 w-old	199922	51856	993	46	9.6
2	XX	8 w-old	69807	20337	605	9	14
3	XX	8 w-old	91630	38606	2101	23	16.9
4	XX	8 w-old	197278	66190	3898	58	15.3
5	XX	8 w-old	126823	46440	3086	44	16.6
Automated Prl;eYFP countings in adult dissociated AL Sox9CreERT2;ReYFP after induction at P0 (grouped/litter)							
Animal	Sex	Age	DAPI	Prl	eYFP	Prl;eYFP	
1	XY	8 w-old	91672	12034	1095	47	
2	XX	8 w-old	89429	12953	1615	91	
1	XY	8 w-old	44111	2978	761	33	
2	XX	8 w-old	53567	7816	1353	74	
1	XY	8 w-old	83669	8973	1330	3	
2	XX	8 w-old	43500	6159	359	1	
3	XX	8 w-old	47918	5282	463	2	
4	XX	8 w-old	66781	9894	305	3	

Figure 6E, F countings

Supplementary Table 5

CELL.SIGNATURE	GENE
Lactotroph	Prl
Lactotroph	Myoc
Lactotroph	Drd2
Lactotroph	Pou1f1
Somatotrophs	Gh
Somatotrophs	Ghrhr
Somatotrophs	Pou1f1
Thryotrophs	Tshb
Thryotrophs	Trhr
Thryotrophs	Dio2
Thryotrophs	Cga
Melanotrophs	Pomc
Melanotrophs	Pax7
Melanotrophs	Tbx19
Melanotrophs	Pcsk2
Corticotrophs	Crhr1
Corticotrophs	Tbx19
Corticotrophs	Pomc
Corticotrophs	Avpr1b
Gonadotrophs	Lhb
Gonadotrophs	Fshb
Gonadotrophs	Gnrhr
Gonadotrophs	Cga
Gonadotrophs	Nr5a1
Gonadotrophs	Foxp2
Endothelium	Cdh5
Endothelium	Angpt2
Endothelium	Pecam
Pericytes	Pdgfrb
Pericytes	Cspg4
Pericytes	Acta2
Macrophages	Cd68
Macrophages	Cd14
Macrophages	Ccr5
Stem cells	Sox2
Stem cells	Sox9
Stem cells	Hes1
Stem cells	Hey1
Stem cells	Fgfr1
Stem cells	Notch1